applied sciences

MDPI

Article

Numerical Design and Analysis of Advanced Roof Systems in Architecture with Environmentally Friendly Low-Carbon Materials

Faham Tahmasebinia [1,*], Wenxi Zeng [1], Bernadette Macaraniag [1] and Krzysztof Skrzypkowski [2,*]

[1] School of Civil Engineering, The University of Sydney, Sydney, NSW 2008, Australia; wzen5427@uni.sydney.edu.au (W.Z.); bmac8679@uni.sydney.edu.au (B.M.)
[2] Faculty of Civil Engineering and Resource Management, AGH University of Krakow, Mickiewicza 30 Av., 30-059 Kraków, Poland
* Correspondence: faham.tahmasebinia@sydney.edu.au (F.T.); skrzypko@agh.edu.pl (K.S.)

Abstract: This research explores the viability of bamboo as a green replacement for timber in building practices. Bamboo's advantages lie in its renewability, sustainability, and resilience to disasters, despite possessing mechanical properties similar to timber. The study proposes using Finite Element Analysis (FEA) simulations, a potent instrument for designing and analyzing intricate structures under varying loads. The research explicitly employs FEA simulations to examine the application of bamboo in complex rooftop systems, using two commercial 3D CAD software—Rhino7 and Strand7. Rhino7 is responsible for 3D model creation and the member's division into minuscule elements, whereas Strand7 is used to assign material properties, establish boundary conditions, carry out simulations, and analyze the outcomes. This research includes case studies of bamboo grid-shell structures and implements the suggested methodology. The study's objective is to augment the scarce engineering data and to analyze bamboo as a material and the impact it can have on construction. The study's results underscore the potential of eco-friendly, low-carbon materials, such as bamboo, in the construction industry. It also illustrates the effectiveness of FEA simulation in analyzing elaborate structures.

Keywords: sustainability; bamboo structures; Strand7; architectural design; low-emission materials; finite element analysis; grid-shell construction

Citation: Tahmasebinia, F.; Zeng, W.; Macaraniag, B.; Skrzypkowski, K. Numerical Design and Analysis of Advanced Roof Systems in Architecture with Environmentally Friendly Low-Carbon Materials. *Appl. Sci.* **2024**, *14*, 2041. https://doi.org/10.3390/app14052041

Academic Editor: Young-Hum Cho

Received: 31 January 2024
Revised: 19 February 2024
Accepted: 22 February 2024
Published: 29 February 2024

1. Introduction

The building and construction industry constitutes up to 78% of greenhouse gas (GHG) emissions globally, majorly affecting the public [1]. The significant rise in GHG emissions is due to the rapid urbanization in response to the increasing demand of building infrastructure and population growth. In fact, 39% of global carbon dioxide emissions are attributed to buildings, partly due to energy consumption (18%), embodied emissions (11%), and direct or operational carbon emissions from the use of fossil fuels (10%) [2].

Embodied carbon emissions are determined by the lifecycle of construction materials in building infrastructure from material processing, transportation, and manufacturing to maintenance during use [3]. A plethora of studies exploring the decarbonization of buildings have confirmed that the consideration and analysis of material behaviors, especially during the development stages of design, are integral to reducing embodied carbon by up to 45% [3].

Sustainability and renewability are significant in combating carbon emissions and understanding the material composition also helps in reducing the subsequent energy consumption and operational carbon. Low-emission materials, including bamboo, timber, and recycled brick, among others, were identified to play a significant role in the decarbonization of buildings.

Bamboo is classified as a low-carbon material, since it consumes less energy to manufacture and is used in construction for its capabilities to absorb large quantities of carbon dioxide (CO_2) from its surrounding environment [4]. Largely recognized for its flexural strength and rapid growth rate, the mechanical properties of bamboo are comparable to timber when treated or engineered. In fact, it is claimed that engineered bamboo has twice the compressive strength of engineered timber, making it a potential contender in modern construction [5].

Yet, due to its anisotropic and non-homogenous properties, there are notable variations in longevity, structural capacity, and quality between bamboo species, determined by the climate and weather conditions in their harvesting locations [5]. These conditions can affect the uniformity of the cross-sectional area and fibers, influencing the mechanical performance between species. The nodal structure of bamboo also introduces variations in material thickness, and therefore, stiffness [5]. This continues to pose a challenge in standardizing the structural behavior and durability of bamboo in construction with more than 1500 bamboo species worldwide to account for [6]. To date, no design standards specific for bamboo structures have been published [7].

However, as a compelling subject, a plethora of studies continue to investigate the properties of bamboo in complex architecture and structural scenarios and emphasize its value in climate change mitigation.

This study aims to assess the structural potential of bamboo in complex grid-shell architecture, highlighting its value as a low-emission material in construction. Two explorative bamboo grid-shell roof designs will be presented and assessed using Finite Element Analysis (FEA) in Strand7, using a set of preliminary design guidelines proposed for the bamboo varieties.

2. Literature Review

2.1. Low-Carbon Materials

Building materials classified as 'low-carbon' possess material properties that lower their embodied carbon emissions and reduce their environmental impact during manufacturing and building construction. Embodied carbon is governed by a material's durability over time and its involved manufacturing processes, whereby the use of fossil fuels is most common, particularly in treating timber materials [8].

Recent studies have shown that the use of low-carbon materials can reduce the carbon emissions from the manufacturing process of building materials more than 20%. This reduces the overall carbon footprint of building designs by lowering fossil fuel consumption by 1.5% [9]. Particularly plant-based materials such as bamboo, can absorb carbon dioxide, improve air quality, and reduce overheating [10]. This can lower the direct emissions involved in heating and cooling systems during the building's operational stage by facilitating thermal comfort through passive design. For example, the use of low-carbon timber can reduce embodied carbon emissions by up to 35% during use, lowering overall carbon emissions by 32% throughout the building's life cycle. This can be estimated through a product life cycle analysis (LCA), which predicts the carbon emissions due to energy consumption and manufacturing [11].

2.2. The Value of Low-Carbon Materials in the Construction Industry

Major studies have shown the value of low-carbon materials in addressing concerns of excessive carbon emissions in the construction industry. Excessive GHG emissions are attributed to the magnitude of waste produced due to poor decision making, such that 10–30% of landfill is construction waste, comprising chemical and combustible material [12]. With limited applications of low-carbon materials in modern architectural and engineering designs, the goal for decarbonization by 2050 is unlikely to be met. The 2019 Global Status Report has verified that, due to rapid urbanization, sustainable building practices, including considerations of low carbon emissions, are falling behind the increasing demand of building services, population growth, and energy demands [12]. In 2022, only 1.6%

of carbon emissions were reduced by current building practices [13], which requires a further 49% reduction in carbon emissions by 2030 to achieve the goal of net zero carbon by 2050 [13].

These insights further highlight the value of low-carbon materials in construction to reduce carbon emissions and to achieve the existing environmental goals of net zero carbon. This can include improved thermal comfort, longevity, and reduced environmental impact, as further explored in the designs proposed in this study. Yet, while research emphasizes the beneficial contribution of low-carbon materials in construction, there are no known specialists with knowledge on low-emission materials, and fewer resources are accessible to the market [14].

This background review motivates the objectives of the conceptual design: to investigate the limitations of bamboo in complex roof systems and encourage further complex applications of bamboo construction in engineering and architectural design. In this way, this study aims to contribute to the study of bamboo as an alternative material to timber and prompt further investigation into low-carbon materials in future structural designs.

2.3. Bamboo in Structural Design and Construction

Bamboo construction is one of the oldest forms of fabrication [10]. Generally defined as a lightweight and renewable material, the popularity of bamboo construction is due to its versatility in building design, both in raw and processed form [15]. Natural or raw bamboo has a circular hollow section demonstrating high rigidity under tension and a greater resistance to torsional effects [7]. Bundles of two–five culms of bamboo are used to increase the lateral stability in building design, whereby the perpendicular stresses are evenly distributed between the bundled bamboo stems [15]. The length of these culms is determined by the spacing between nodes in bamboo members. The nodal structure of bamboo stems results in a non-uniform circular hollow section due to the increased thickness, and therefore rigidity, at these nodes [7].

2.4. Materials Properties

Bamboo belongs to the poaceae or grass family, similar to rice, corn, and sugarcane. The lignin in bamboo tissue is what enhances its strength, while retaining a flexible and lightweight quality [16]. The bamboo structure consists of a hollow cylindrical culm, which is divided into sections by nodes [17]. The structure of bamboo is considered to be more heterogeneous than that of wood [18]. This is explained in Figure 1.

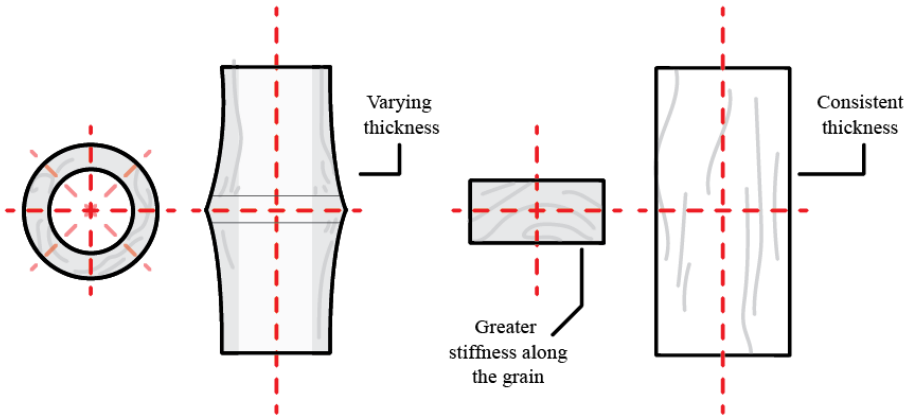

Figure 1. Isometric of a bamboo culm (**left**) and isometric of timber beam (**right**) showing a similar composition in the direction of the fibers/grain, though with different cross-sections.

As mentioned previously, the physical and mechanical properties of bamboo species are determined by their harvesting location in terms of climate, topography, soil type, altitude, age, stem, and humidity [16]. Physical variations can include the culm diameter, ranging from 0.64 cm to 30.48 cm, and total length, ranging from 0.30 m to 37 m [19]. These

physical differences can enable an opportunistic structural approach, sourcing multiple species for one structure as a combined system. This is demonstrated by the precedent studies presented in Section 2.8. Mechanical variations between species determine the stiffness of the bamboo, whereby the axial or compressive strength can vary between approximately 5 and 25 GPa, and the tensile strength can vary between 100 and 800 MPa [20–22].

The above properties are typical for raw, untreated bamboo. Recent studies show that treated and engineered bamboo provide an opportunity to maintain the structural capacity and durability of raw bamboo, through the combination of culm fibers to produce strengths greater than timber, as shown in Section 2.5.

2.5. Comparison of Raw Bamboo and Bamboo Scrimber

A short comparative study of two common bamboo materials—raw bamboo and bamboo scrimber—provides an insight into the above, as listed in Table 1.

Table 1. Comparison of raw bamboo and bamboo scrimber properties.

	Raw Bamboo	**Bamboo Scrimber**
Material Properties	Anisotropic and non-homogeneous	Isotropic and homogeneous
Cost	In-expensive	Larger due to manufacturing
Curvature	Harder to form curves	Easier to form curves
Density ρ (kg/m^3)	666 [9]	1010
Compression f_c (Mpa)	53 [9]	134.9
Tension f_t (Mpa)	153 [9]	296.2
Shear τ (Mpa)	16 [9]	15
Flexural f_b (Mpa)	135 [9]	119
Elastic Young's Modulus (GPa)	15 [9]	22.9
Poisson's Ratio	0.52 [9]	0.22

Raw bamboo is the natural, untreated species more traditionally used as a construction material for basic habitats to complex structures [16].

Bamboo scrimber, on the other hand, is a composite material that maximizes the mechanical properties of natural bamboo by processing and treating the crushed bamboo fibers with truncation, splitting, drying, assembly, cold-pressing, and heat-curing or hot-pressing. These bundled fibers are laminated using resin, maintaining the longitudinal strength in raw bamboo [23]. It is typically provided as prefabricated slats, which eliminates the cross-sectional variability common in raw bamboo [24].

Bamboo scrimber possesses twice the compressive and tensile strength as raw bamboo [24], despite having similar flexural and shear capacities. While bamboo scrimber may perform significantly stronger in design when compared to raw bamboo, it is more costly, as it requires additional treatment and processing [23].

For the purpose of this study, the properties of raw bamboo will used. In future studies, we recommend analyzing the mechanical performance of bamboo scrimber.

For raw bamboo, many high-quality bamboo resources have not been effectively developed, especially for some clumping bamboo species in Southeast Asia and South Asia. Clumping bamboo is a preferred species for construction, due to its density and easy harvest. *Thyrsostachys oliveri* is one tropical example. As a moderately large clumping bamboo with long-spanning culms, it possesses the closest properties to homogenous materials when compared to Moso bamboo *Neosinocalamus affinis*, and other clumping bamboos [25]. It is noted that no sufficient structural data have been published for this species. The following properties in Table 2 will be used for the Stand7 analysis in Section 3.

Table 2. Material properties.

Property	Value	Units
Density (ρ)	666 [9]	kg/m^3
Elastic Modulus	15 [9]	GPa
Poisson's Ratio	0.46 [9]	-
Diameter (D)	0.07 [24]	m
Thickness (t)	0.012 [26]	m

2.6. Connections and Joinery Techniques

As bamboo has a circular hollow section, particular joinery techniques are required to maximize its structural capacity. The most common bamboo connections, especially those observed in vernacular construction, include 'fish mouth' joints, lashings, plug-in joints, and positive-fitting connections [27]. These techniques use friction between the bamboo members to counteract the torsional stresses and reduce the splitting of the fibrous material.

A common, and more modern, articulation of the lashings or fish-mouth joint are those using bolded connections or internal connectors between the nodes and culms of bamboo members. These internal connections are most suited to reducing the perpendicular stresses that may 'crush' the bamboo [27]. This study will consider rigid connections between interlocking bamboo members using two joint types: bundling with bolted connections and the mortise and tenon craft techniques, as shown in Figure 2. The base connections to the ground will be assumed to be fixed to concrete piers using steel connections and are defined as rigid connections.

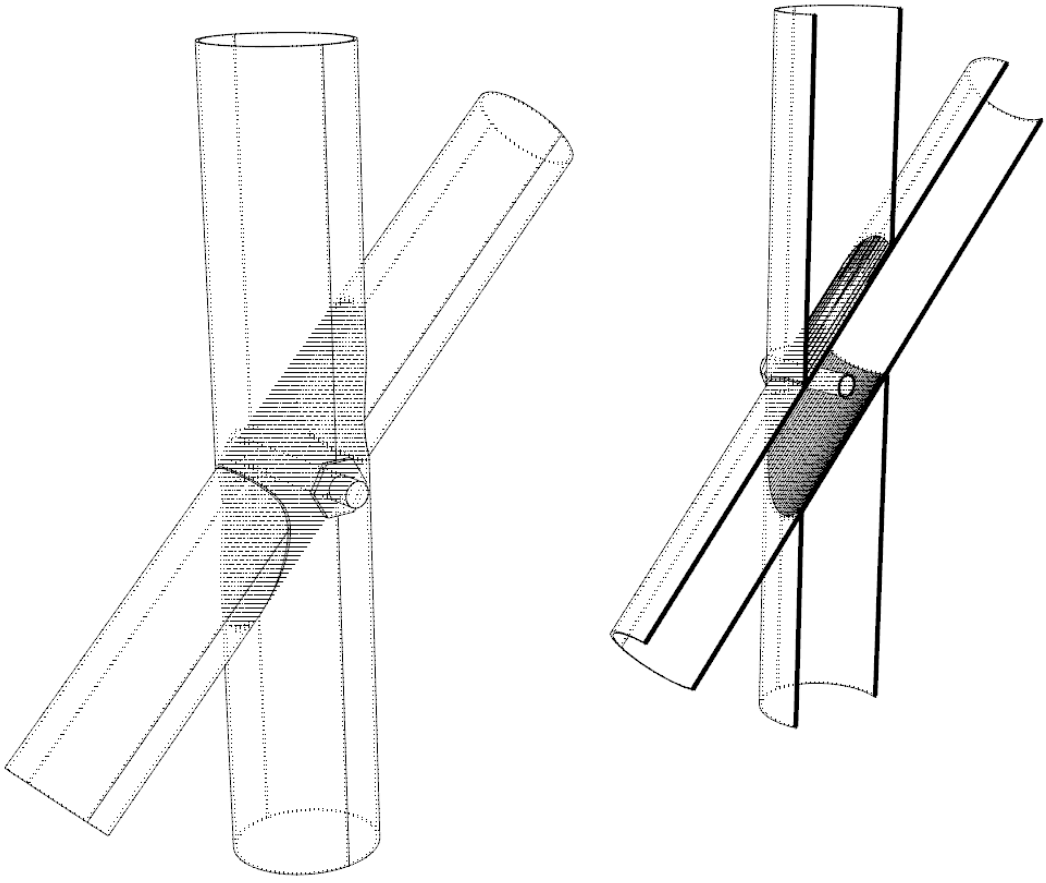

(**a**)

Figure 2. *Cont.*

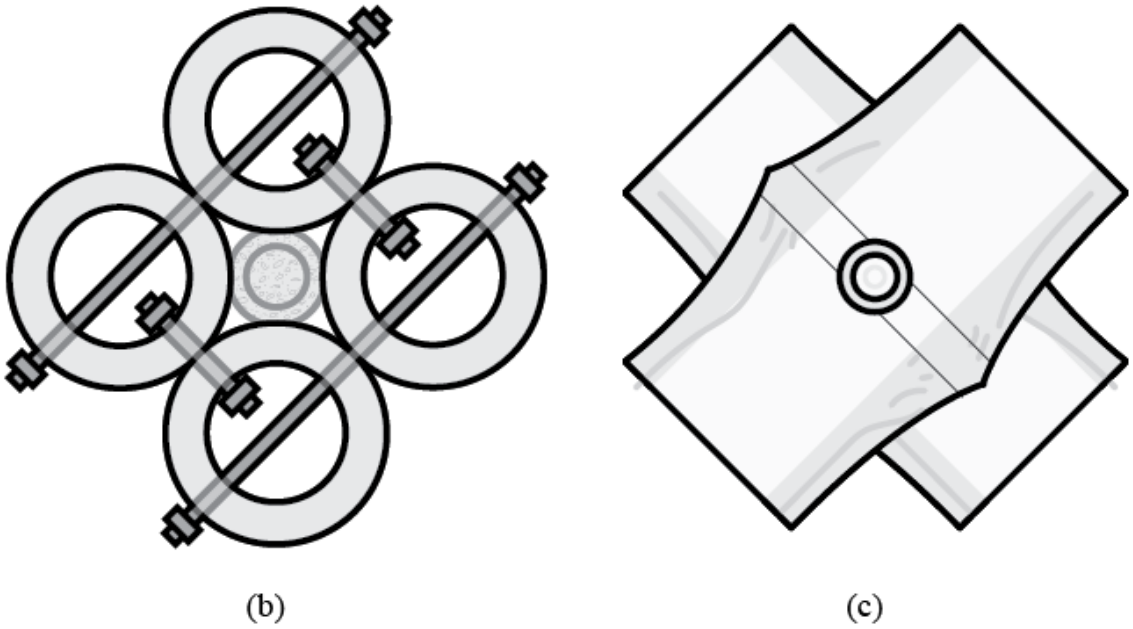

Figure 2. Bamboo connection by the mortise and tenon joint (**a**,**c**) and bundling with bolted connections (**b**).

2.7. Grid-Shell Design with Bamboo

Grid-shell structures are known to be more cost-effective and efficient with longer spans using less materials than the standard structural counterparts. Especially used in low-rise architecture, the structural performance of grid shells is attributed to their 'woven' aspect, allowing for a two-way span structure. This enables increased rigidity without vertical support, establishing greater possibilities with designs across various contexts, including housing, pavilions, and facades [28]. The two-way spans of a grid-shell structure contribute to its rapid construction and flexural strength, as the fabrication process can easily be achieved on site or through prefabrication. This reduces additional processing costs in transportation and construction by reducing the complexity of assembly [29].

Bamboo grid-shell structures expand the architectural opportunities of larger spanning projects by using lightweight and low-emission materials that would further decrease the environmental impact of such designs [28]. When considering design strategies in congruence to material selection and structural solutions, the reduction in embodied carbon emissions can be significant.

2.8. Precedent Studies of Existing Bamboo Grid-Shell Structures

Grid-shell bamboo architecture has been widely used for large-spanning structures, such as a gymnasiums and school halls. Evidently, designers utilize the flexibility and strength of bamboo through bundling bamboo stems and the layering of individual stems to increase the cross-sectional capacity of certain structural components of the building. Three precedent studies have been conducted to observe the existing solutions of bamboo grid-shell structures and to observe the structural actions and methodology which optimize the flexural strength and adaptability of bamboo as an architectural and structural material. As preliminary studies, the structural system and design philosophy of these buildings were observed at a high level and will influence the conceptual designs presented in Section 3.

2.8.1. Panyaden International School by Chiangmai Life Construction

The Panyaden International School Sports Hall in Chiang Mai, Thailand, was designed using bamboo to be cohesive with the existing facilities of the school. Inspired by the shape language of the lotus flower in order to align with the school's spiritual beliefs, the

grid-shell design maximizes the flexibility of the bamboo material to establish a large open space with optimal ventilation and natural lighting. The exposed bamboo structure also allows for breathability in the sports hall and further contributes to the spatial experience from the interior to the surrounding landscape [29].

The presentation of the bamboo construction forms a major part of the design's example for bamboo grid-shell designs. Using prefabricated trusses of bundled bamboo culms, the structure spans over 17 m. These bundled culms are treated and tightly bound by rope, celebrating the handicraft of traditional bamboo structures within Thailand. Simultaneously, the bundling of the culms increases the lateral rigidity of the bamboo and reduces the occurrence of splitting within the fibers of the members. This further reduces the shearing stresses due to the curvature of the design [30].

The design assigns variable diameters of bamboo members by curvature and strength; thicker bamboo culms are utilized as bracing or supports, while thinner bamboo culms are utilized for harsher curves, such as the openings of the hall. This is further explained in Figure 3.

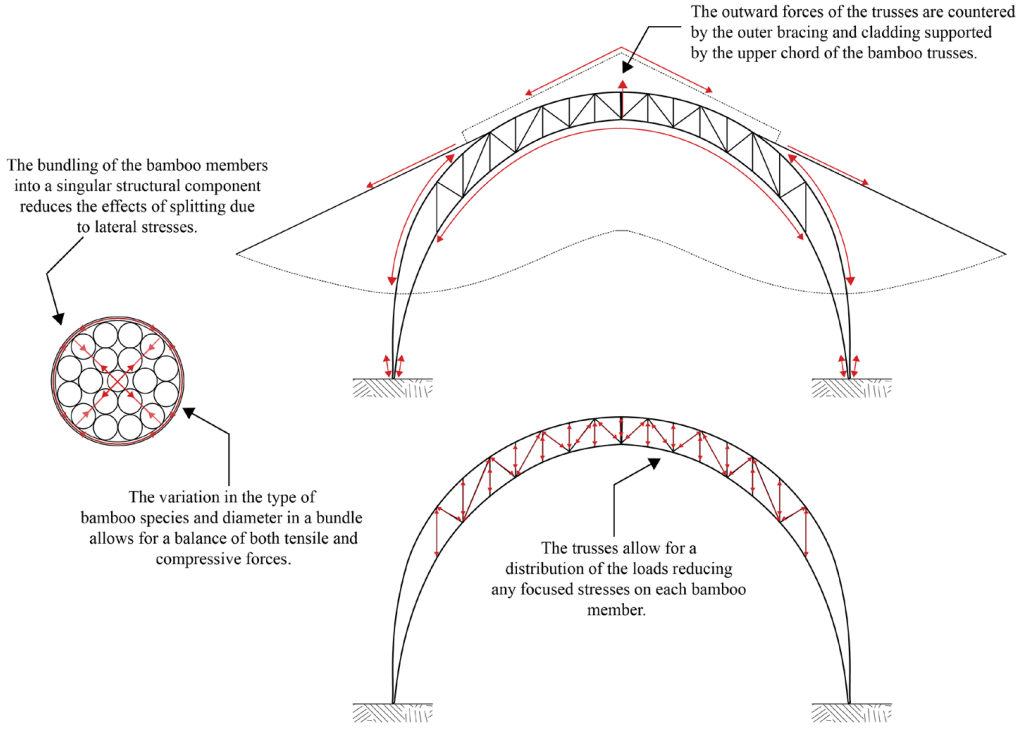

Figure 3. Annotated high-level study of structural actions in design.

2.8.2. The Arc at Green School Bali by Ibuku Bamboo Architecture and Design

The Arc at the Green School in Bali by Atilier One Architects presents an alternative perspective on bamboo grid-shell structures. The design's primary focus on efficiency and simplicity in structural form further emphasize the versatility of bamboo in its strength and shape for large spanning structures. While steel connections are used to bundle the bamboo culms, the structure is predominantly constructed with bamboo, such that the cladding and bracing elements of the roof are fabricated from compressed bamboo sheets, using various species to reinforce the durability of the external elements [31].

The weaving design of the structure further unifies the design as a single system, facilitating a cohesive form that evenly distributes the loads and combined actions.

In combination with existing concrete foundations, the strength of the bamboo culms is reinforced by the resistance of thicker bamboo stems with larger cross-sectional areas, reducing the effects of torsional and lateral stresses due to the curvature of the roof. This can be further observed in Figure 4.

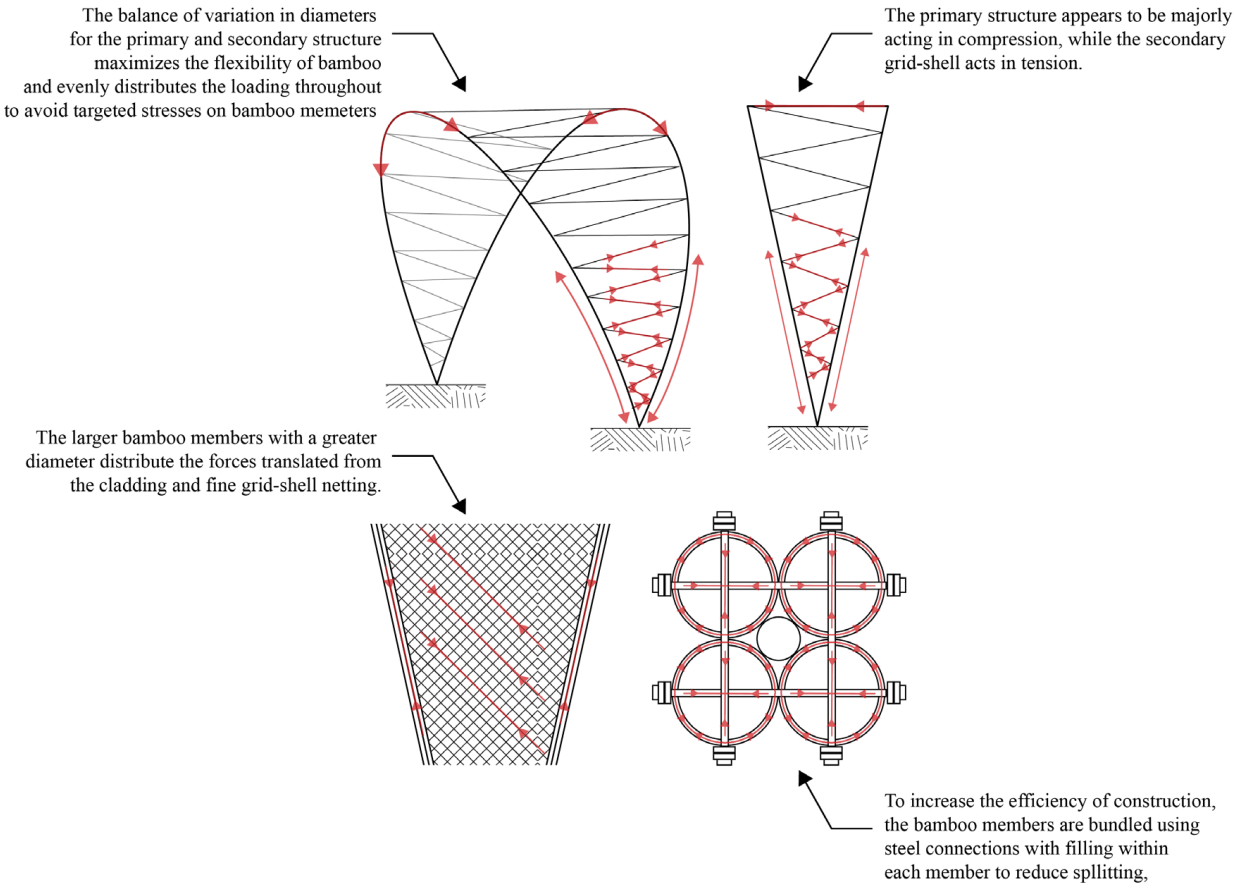

Figure 4. Annotated high-level study of structural actions in design.

2.8.3. Nonenco Café by VTN Architects

Located in Vinh, Central Vietnam, the Nonenco Café by VTN Architects is a prime example of maximizing the structural and flexural properties of grid-shell bamboo structures through bundling bamboo culms. VTN Architects selected bamboo as a primary material for their structure, due to its ease of construction, affordability, and the accessibility to tropical environments. Providing a unique identity to the design, as described by VTN Architects, bamboo, in the context of Central Vietnam, brings contrast to the re-establishment of European architecture. Beyond exploring the structural capacity of bamboo, Nonenco Café is a particularly great example for demonstrating the versatility of bamboo structures in different structural formations, including dome structures and cave-like and rectilinear configurations. As shown in Figure 5, the Roof Top Club floor demonstrates combined actions through a series of arches and complex curvatures to imitate a cave-like formation [32].

By increasing the sectional capacity of each contributing component of the bamboo roof, the design maximizes the flexural rigidity of the bamboo members, minimizing the torsional stresses at the connections through layering and through the careful arrangement of the bundled components. This design highlights that the strength of a bamboo structure is determined by the effectiveness of the connections. The circular cross-sectional area poses challenges for the connections between stems without compromising the sectional capacity of the bamboo stems. Nonenco Café evidently uses layering to mitigate these effects. This is further detailed in Figure 5.

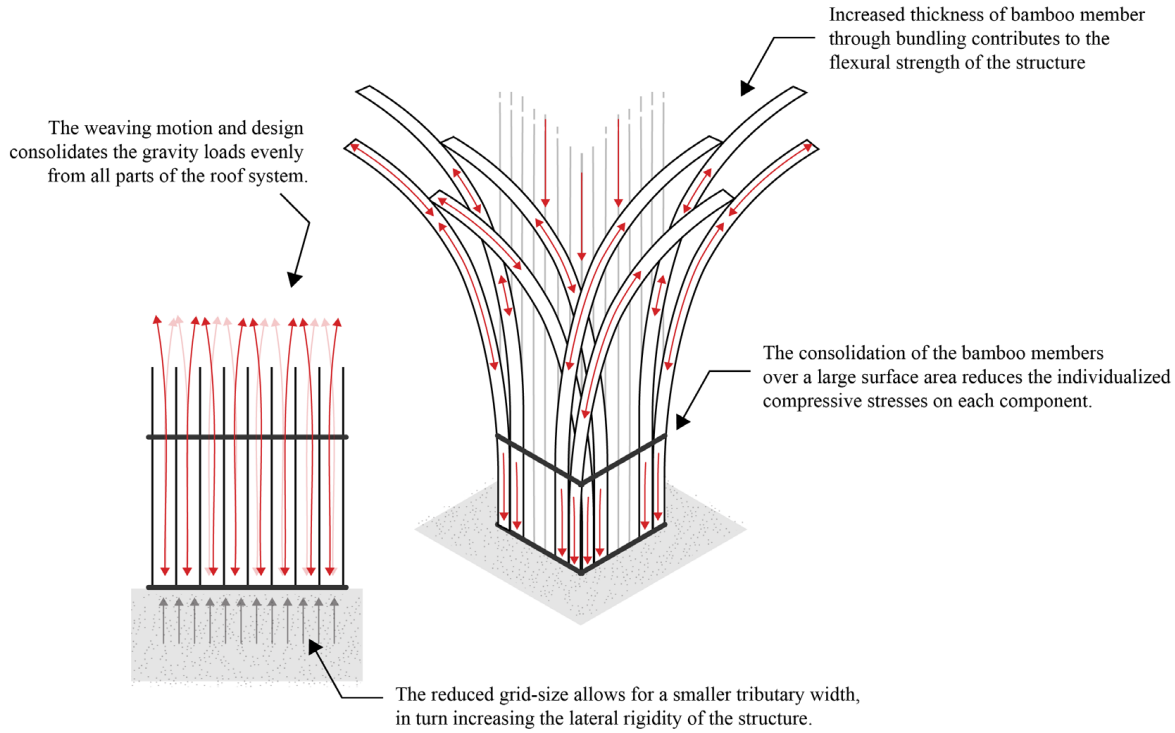

Figure 5. Annotated high-level study of structural actions in design.

3. Case Studies of Bamboo Grid-Shell Structures

3.1. Introduction

Two preliminary designs of bamboo grid-shell roof structures are presented below. Each design presents a different architectural approach to the use of bamboo in construction. These designs will be introduced with the opportunity to optimize their structural intentions according to the behavior of the bamboo in each context. The designs will be assessed in Strand7, using the three-dimensional models produced in Rhino 7 with Grasshopper. Three iterations of each design will be produced to present these findings.

3.2. Design Case Study One—Buddhist Lotus Shelter

The first case study considers rotational symmetry to optimize the structural capacity of raw bamboo. The Buddhist Lotus Shelter maximizes the flexibility and resilience of bamboo to produce a long-spanning shelter of up to 10 m that is centralized around the users, taking inspiration from the natural sequence in floral arrangements. A visual rendition of this design is shown in Figure 6a. The design takes interpretive elements from Buddhism to also inform its architectural strategies, such as thermal comfort and lighting, as summarized below:

- Natural cooling and centralized lighting through a small opening located at the apex with reduced noise pollution via plywood cladding.
- Increased structural rigidity by the intersecting of bamboo stems.
- Even distribution of gravity loads by rotational symmetry. Increased lateral stability and structural rigidity by rotational symmetry and connections, as shown in Figure 6b,c.
- Reduced torsional effects by the catenary action of bamboo members.

The design is heavily inspired by the significance of the lotus flower, symbolizing beauty and tranquility [33], and the resilience of bamboo, as represented in common art forms of traditional Chinese culture. The natural geometry of the floral patterns governs the purpose of the architecture, establishing a harmonious space that celebrates the simplicity of the structure and strength of the bamboo.

Three iterations of this design are presented below, with the intention of assessing the mechanical performance of raw bamboo based on the grid spacing of the grid-shell structure. A structural analysis of this case study is conducted in Section 3.5.

(**a**)

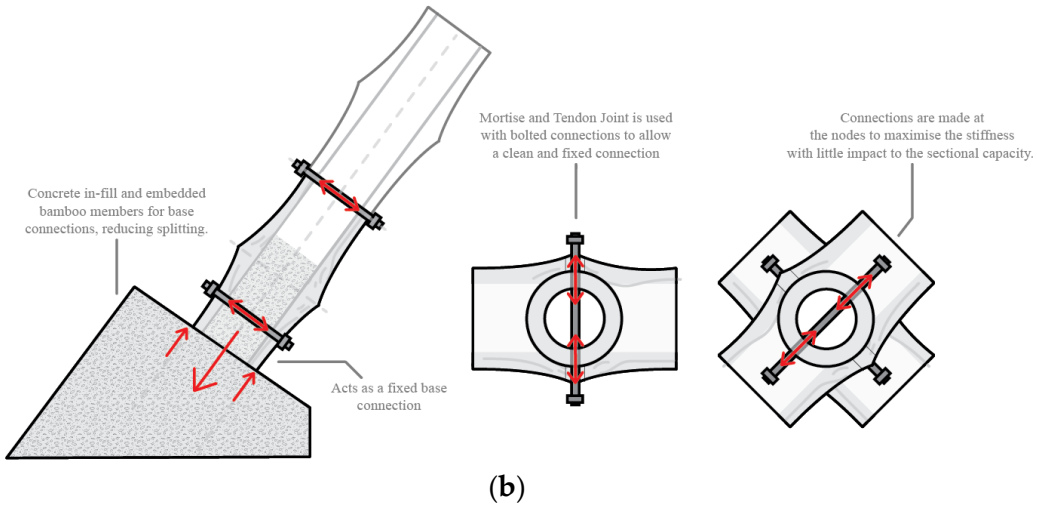

(**b**)

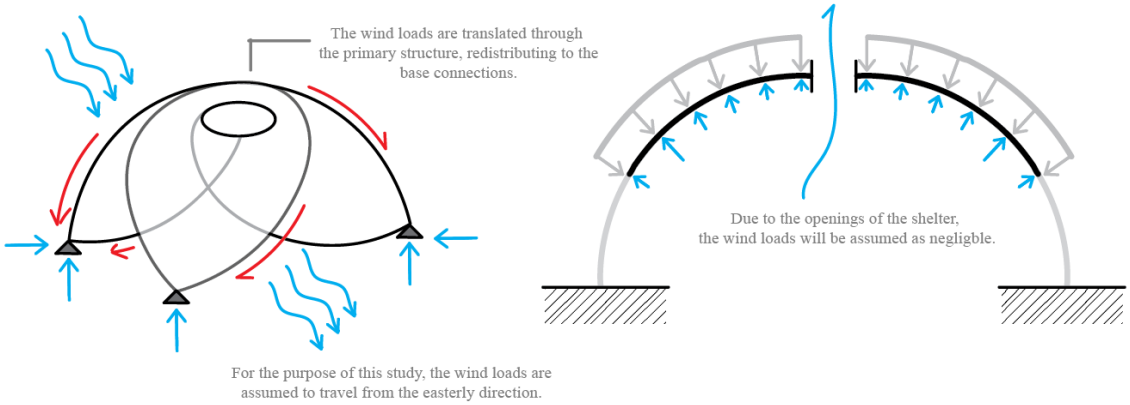

(**c**)

Figure 6. Visualization of the architectural concept for the Buddhist Lotus Shelter (**a**): detailed connections (**b**) and wind load considerations (**c**).

3.2.1. Design Iteration One

The initial design is shown in Figure 7, whereby the shelter is a two-way spanning structure of 10 m in both directions with a height of 3 m. This design utilizes a grid spacing of 1.8 m between bamboo members. All intersecting bamboo members are assumed to be fixed connections up to the apex. The interlocking members to the apex of the structure are assumed to be a pinned connection.

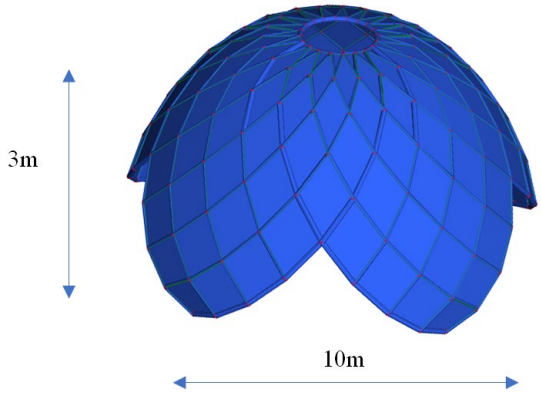

Figure 7. Elevation and plan view of Design Iteration One.

3.2.2. Design Iteration Two

The second design iteration is shown in Figure 8b, where the grid spacing is increased to 4.9 m, twice of the initial design.

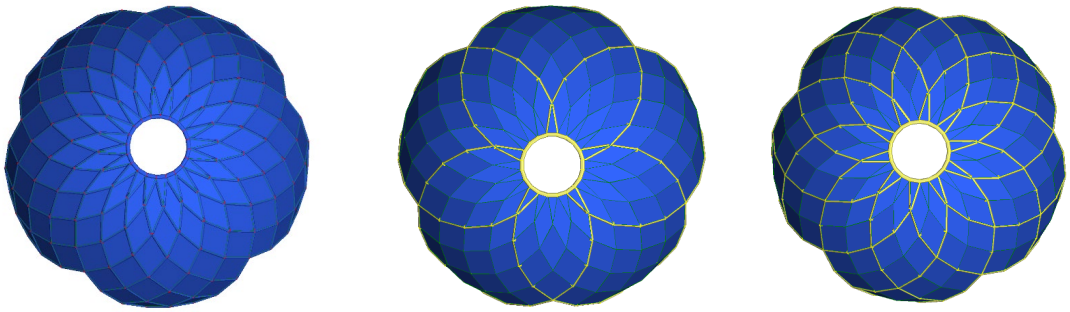

Figure 8. Visualization of Design Iteration Three (**c**) in comparison to previous iterations (**a**,**b**).

3.2.3. Design Iteration Three

The third design iteration in shown in Figure 8c, where the grid spacing is increased to 5.3 m.

3.3. Design Case Study Two—Community Pavilion

The second case study considers bilateral symmetry to optimize the structural capacity of raw bamboo. The community pavilion similarly maximizes the flexibility and strength of bamboo through catenary action and produces a spanning structure of approximately 7 m, taking inspiration from the simplified geometry of floral arrangements. A visual rendition of this design is shown in Figure 9a. The design takes inspiration from origami and negative space to inform its architectural strategies with an emphasis on spatial experience and lighting, as described below:

- Natural ventilation and cooling through a high ceiling and porous roof structure with a fabric membrane overlay.
- Increased rigidity and lateral stability through layering and bundling bamboo stems, as shown in Figure 9b,c.

- Reduced torsional effects by bilateral symmetry and fixed to the ground using concrete infill at the base.

The design is motivated by the value of community and the adaptability of bamboo in multiple architectural and engineering applications. The consideration of its location within a largely populated urban setting influences the purpose of this architecture, facilitating a synonymous space that encourages participation through communion and expression. It celebrates the malleability of bamboo by allowing a portable design that embraces any community function.

(**a**)

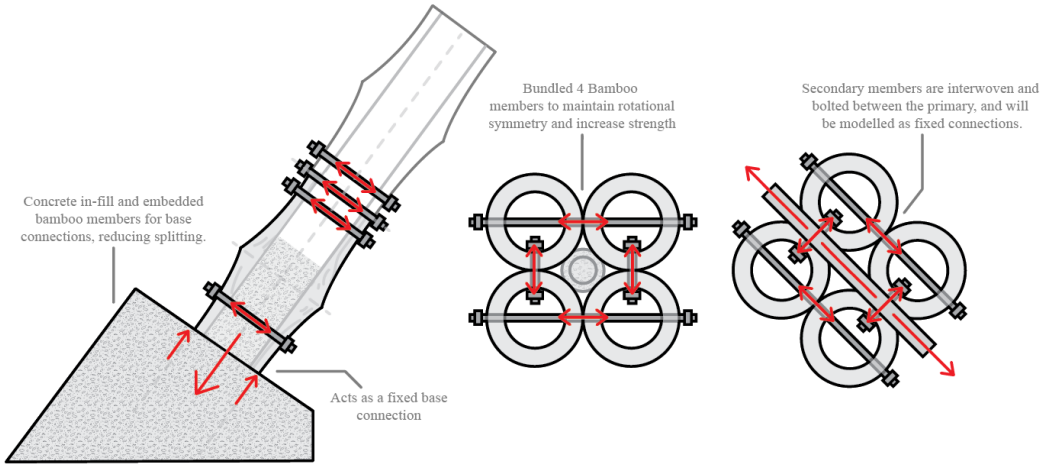

(**b**)

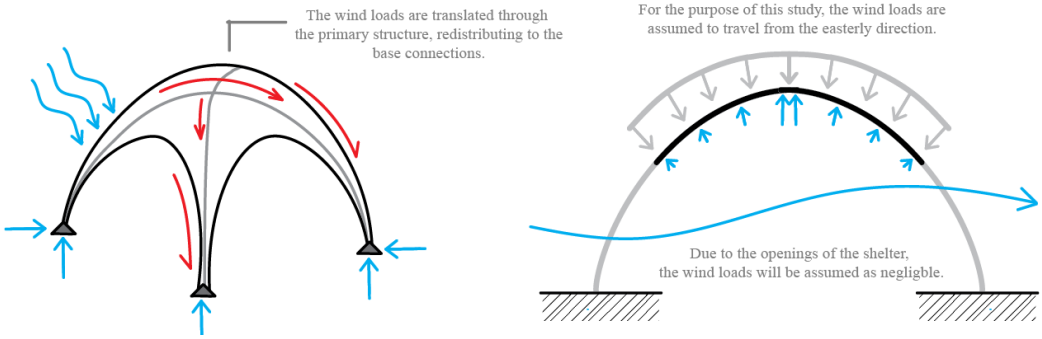

(**c**)

Figure 9. Visualization of the architectural concept for the Community Pavilion (**a**), detailed connections (**b**), and wind load considerations (**c**).

3.3.1. Design Iteration One

The initial design presents a grid-shell structure with a 1.65 m tributary width, as shown in Figures 10 and 11. It will contain two structural components: the bamboo armature (i) and the interlocking bamboo grid-shell stems (ii). This design presents a grid spacing of 1.5 m by 1.5 m, decreasing in size as it approaches the end supports. It is assumed that the end supports are fixed connections, while all intersecting bamboo members are pinned. The connections to the bamboo armature are also assumed to be fixed.

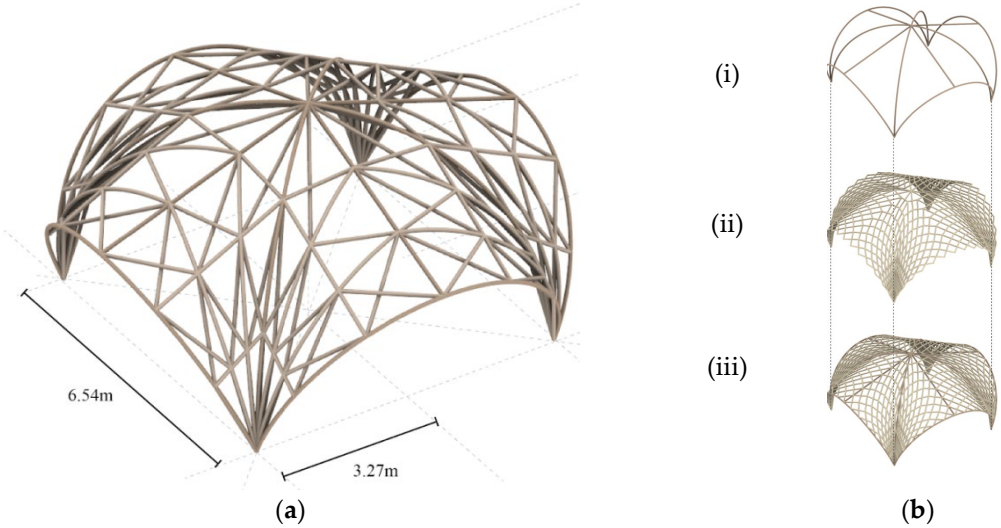

Figure 10. Axonometric model of Iteration One (**a**) with exploded view of structure (**b**).

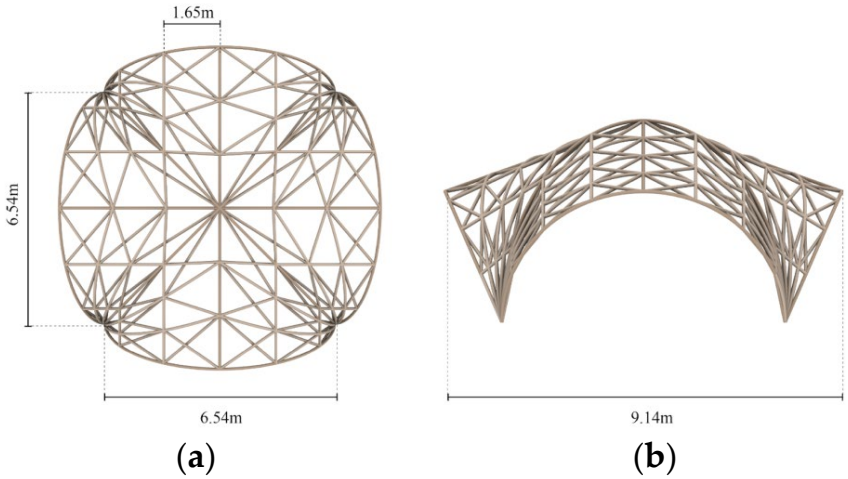

Figure 11. Plan (**a**) and elevation (**b**) view of Iteration Two.

3.3.2. Design Iteration Two

The second iteration presents the developed grid-shell with a 1.23 m tributary width, as shown in Figures 12 and 13. In contrast to the first iteration, the design has improved continuity between the secondary structures, which almost flow with the profile of the roof surfaces. This includes a 1.2 m by 1.2 m grid.

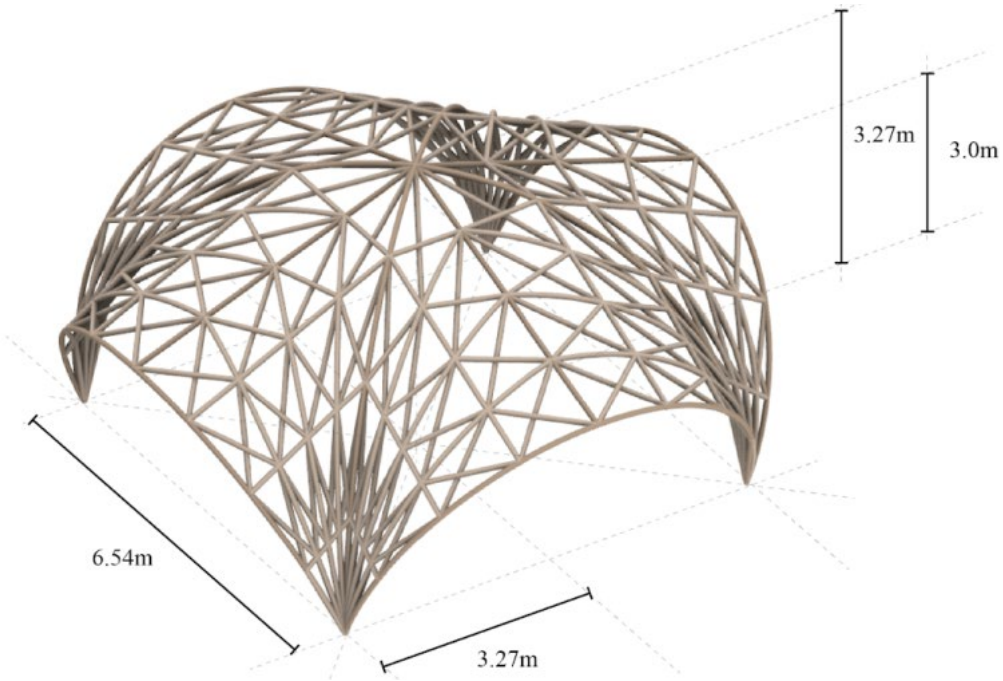

Figure 12. Axonometric model of Iteration Two.

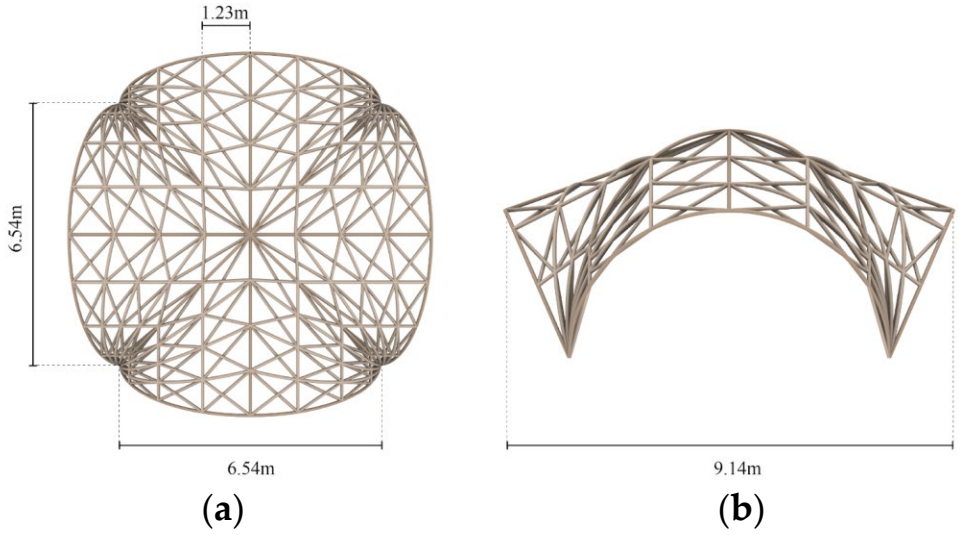

Figure 13. Plan (**a**) and elevation (**b**) view of Iteration Two.

3.3.3. Design Iteration Three

The final iteration presents the initial primary grid shell with a 0.69 m tributary width, which is further shown in Figures 14 and 15. The grid size roughly covers 0.5 m × 0.5 m, where single members of bamboo form the secondary structure. The curvature of the structure transfers all loads and bending moments to the ground more evenly. In comparison to previous iterations, this design presents a more seamless integration of the roof's curvature.

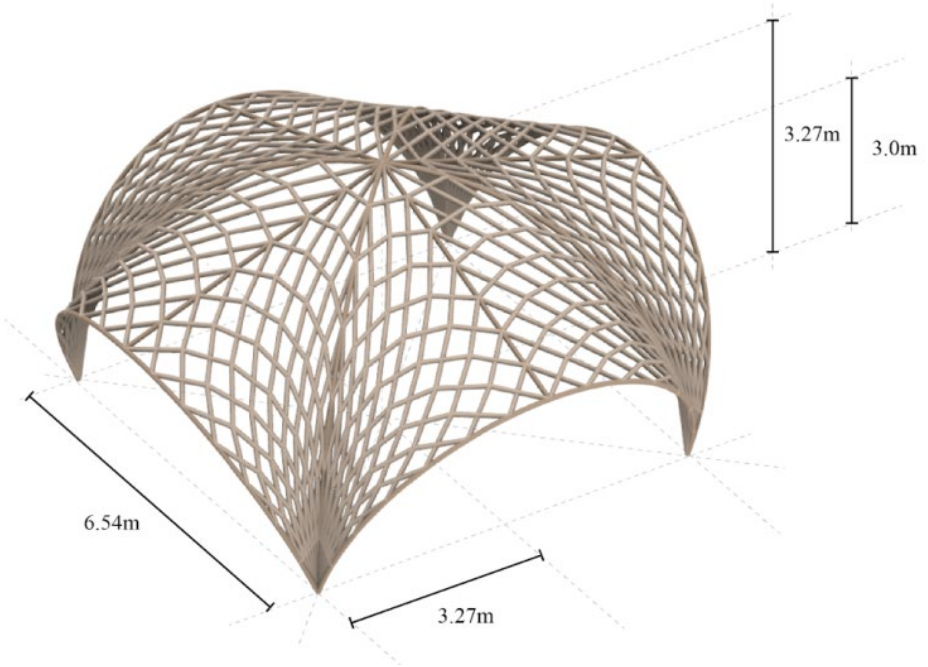

Figure 14. Axonometric model of Iteration Three.

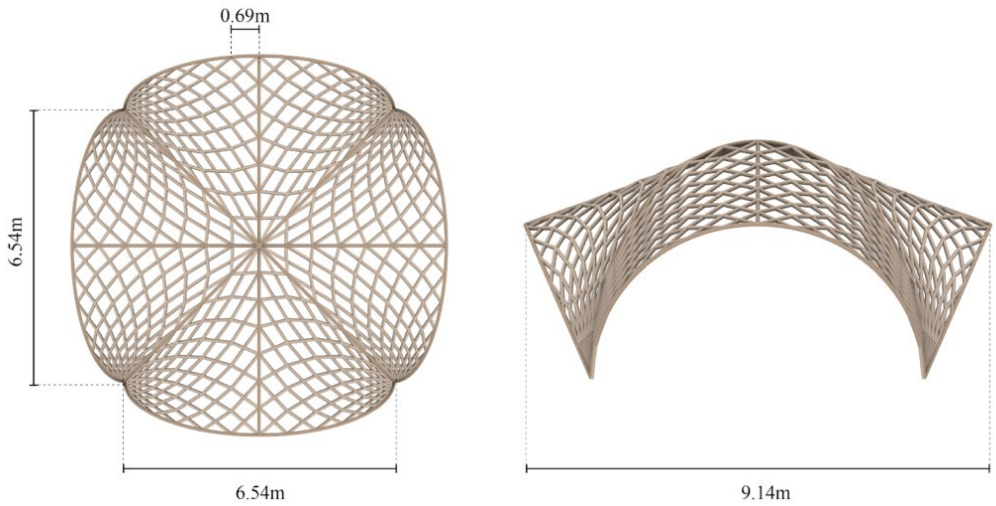

Figure 15. Plan (**a**) and elevation (**b**) view of Iteration Three.

3.4. Modeling for Analysis

As both designs require some form of symmetry, the curvature of the bamboo members and building form were modeled in Rhino7, using a plug-in called Grasshopper, before conducting a FEA analysis in Strand7. Grasshopper is a visual-based coding platform that produces models using a series of parameters, including height, average grid size, and curvature. This allows the iterations to be easily modeled progressively for each conducted analysis. Both designs were modeled according to the following methodology:

1. Massing Model (Rhino7), as shown in Figure 16a.
    a. Creating a profile of the design form's curvature.
    b. Using the Blend tool to create surfaces according to the design curvature.
2. Bamboo Grid Shell surrounding Massing Model (Grasshopper), as shown in Figure 16b.
    a. Divide surfaces into a series of U (horizontal) and V (vertical) points in Grasshopper.

b. Establish the grid size and other parameters to fully map the grid-shell structure on the existing massing model.
c. Create (or Bake) a series of curves that form the grid-shell structure.

3. FEA Model (Strand7), as shown in Figure 16c
   a. Split all imported curves into segments.
   b. Set the connections to the ground and apex as fixed connections.
   c. Run an analysis for the structural assessment.

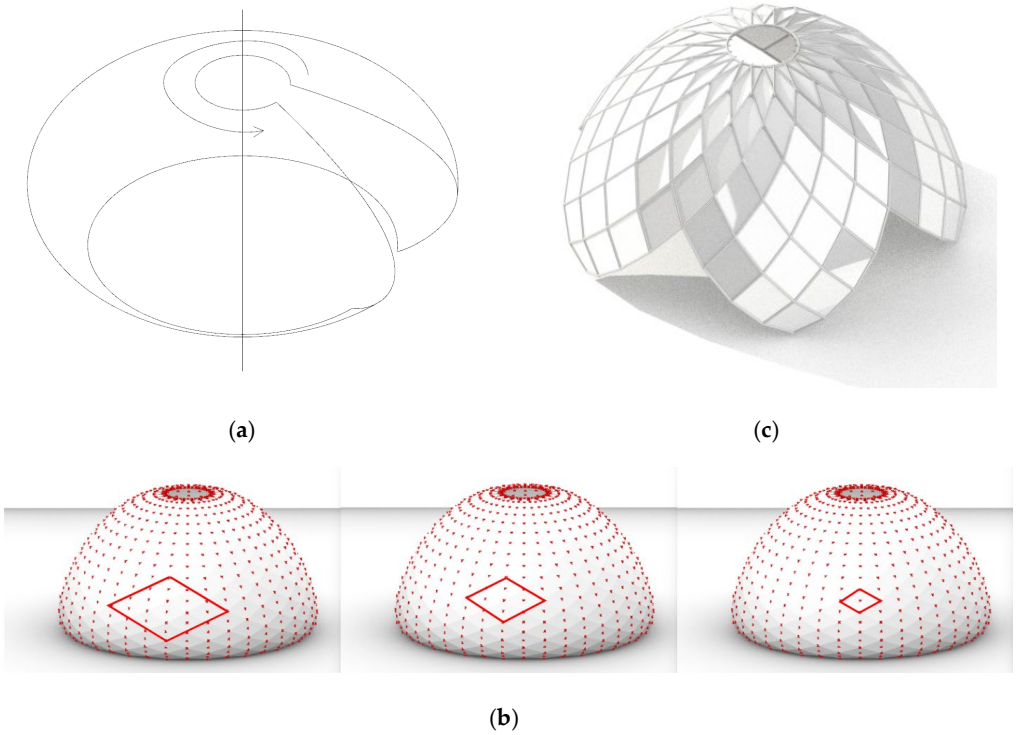

(**a**) (**c**)

(**b**)

Figure 16. Massing model (**a**), divided surfaces (**b**), and structural model (**c**) of Case Study One.

The resulting models for each step are presented in Figures 16 and 17 for each case study. The detailed grasshopper code and breakdown of each design are shown in the Appendices A and B.

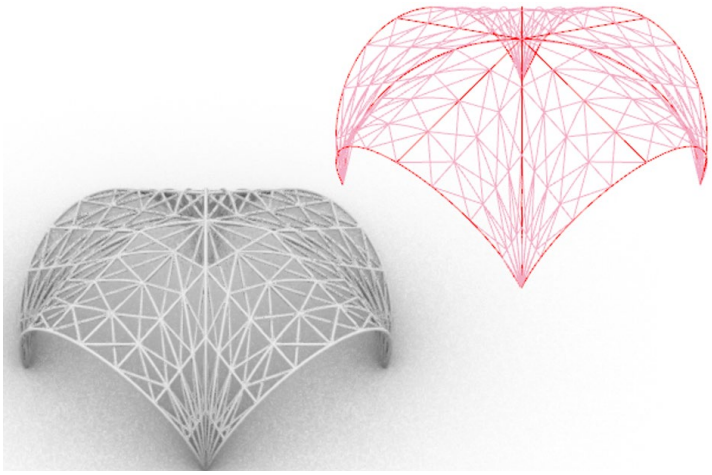

(**a**) (**b**)

Figure 17. Massing model (**a**) and divided surfaces (**b**) of Case Study Two.

3.5. Loading Parameters for Static Load Analysis

To assess the structural capability, the following load conditions are calculated for both designs, according to the following values, as shown in Table 3. The live load was extracted from AS1170.0 [34] and AS1170.2 [35] for typical roof structures as 0.25 kPa, while the wind loads are assumed to be 1 kPa. Since both the bamboo designs are complicated designs with a fluid shape and wide openings, a Computational Fluid Dynamic (CFD) model or a wind tunnel test might be required to simulate the wind effects. The wind load was considered only in the horizontal plane, ignoring the uplifting effects due to the preliminary analysis scope.

Table 3. Values of gravity and wind loads for FEA Analysis.

Load Types	Value	Units
Dead Loads (D) [26]	0.47	kPa
Live Loads (Q)	0.25	kPa
Wind Loads (W)	1.0	kPa

These designs will be assessed according to the loading conditions listed from AS1170.0 [34], as shown in Table 4.

Table 4. Loading Cases to be used for FEA Analysis.

Criteria	Load Combination
Serviceability Limit State	G + Q G + 0.7Q + W
Ultimate Limit State	1.35 G 1.2G + 1.5Q 1.2G + W + Q

It is assumed that the dead loads include the self-weight of the bamboo members and any additional cladding, such that the density is assumed to be 550 kg/m^3. The self-weight of the bamboo members is calculated using the cross-sectional area and density of raw bamboo, as shown below as a uniformly distributed load.

$$A_{bamboo} = \frac{\pi D^2}{4} - \frac{\pi {D_{in}}^2}{4} = 0.0012 \text{ m}^2 \quad (1)$$

$$UDL_{bamboo} = \frac{666 \text{ kg}}{\text{m}^3} \times \frac{9.81 \text{ N}}{\text{kg}} \times 0.012 \text{ m}^2 = 0.008 \text{ kN/m} \quad (2)$$

For the first case study, which uses plywood cladding, the self-weight, using the panel thickness and density, is as calculated below. It is assumed that the typical thickness of the plywood cladding is 19 mm. Hence, its self-weight pressure can be calculated as follows:

$$G_{cladding} = \frac{550 \text{ kg}}{\text{m}^3} \times \frac{9.81 \text{ N}}{\text{kg}} \times 0.019 \text{ m} = 0.10 \text{ kPa} \quad (3)$$

3.6. Structural Design Criteria

Each design will have a different deflection limit, due to the difference in span. The deflection limit is calculated as a ratio of L/250, while the fiber stress limit is calculated according to AS 3600 [36]. However, AS 3600 [36] has only been used for concrete structures. The fiber stress in this preliminary analysis is used to discover bamboo's section performance only when regarded as an isotropic material. Thus, the design criteria for the first and second case study are shown in Tables 5 and 6, respectively.

Table 5. Design Criteria for Case One—Buddhist Lotus Shelter.

Criteria	Limit	Units
Deflection Limit	40	mm
Axial (Compressive) Stress Limit	43.7	MPa
Axial (Tensile) Stress Limit	43.7	MPa
Fibre Stress Limit	26.1	MPa

Table 6. Design Criteria for Case Study Two—Modular Community Pavilion.

Criteria	Limit	Units
Deflection Limit	26.15	mm
Axial (Compressive) Stress Limit	108	MPa
Axial (Tensile) Stress Limit	115	MPa
Fibre Stress Limit	43.5	MPa

For Case Study One, the span of the design is a maximum of 10 m and the deflection limit is calculated as follows:

$$\delta max = \frac{10000}{250} = 40 \text{ mm} \quad (4)$$

Furthermore, based on the axial stress, the fiber stress limit is calculated as follows:

$$\varnothing \gamma_{bamboo} = 0.6 \times 43500 = 26,100 \text{ kPa} \quad (5)$$

For Case Study Two, the span of the design is a maximum of 6.54 m and the deflection limit is calculated:

$$\delta max = \frac{6540}{250} = 26.15 \text{ mm} \quad (6)$$

3.7. Static Load Analysis for Case Study One—Buddhist Lotus Shelter

3.7.1. Design Iteration One

The deformed shapes of the first iteration show concentrated stress at the base connections to the ground and at the highest point of each opening, as shown in Figure 18. The loads are more evenly distributed throughout the bamboo stems, only showing the largest deformation, similarly, at the base connections. This reduced loading on the bamboo is attributed to the plywood plates sustaining the lateral loading. Figure 19 shows the fiber stresses along the cross-sectional area, experiencing a maximum tensile force of 1580 kPa and a maximum compressive force of 2073 kPa.

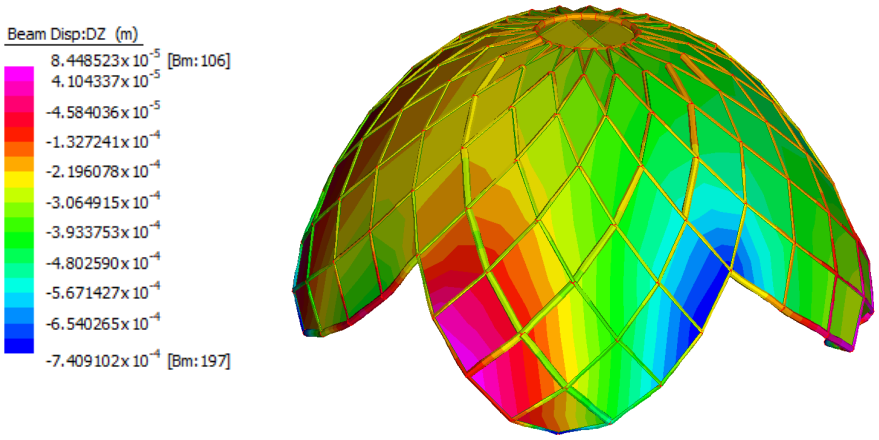

(**a**)

Figure 18. *Cont.*

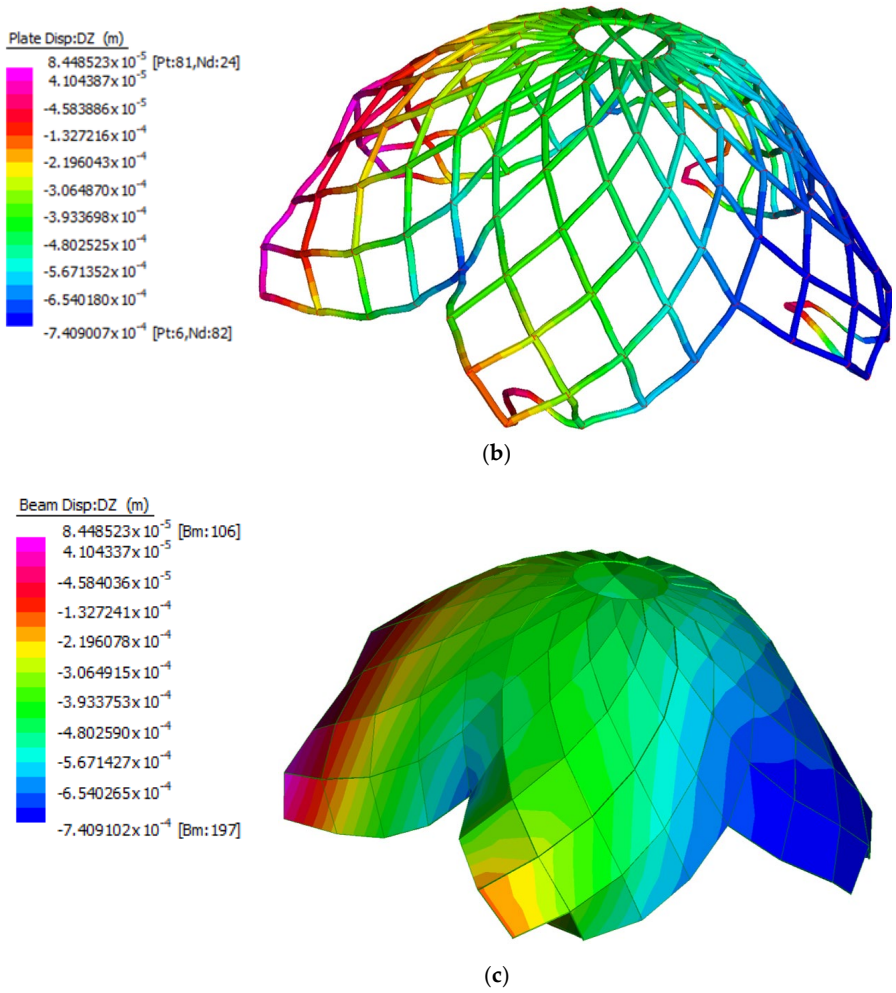

Figure 18. Strand7 analysis of Case Study One—Iteration One showing the deformed shape of the combined structural system (**a**). An isolated analysis was conducted for the structural beams (**b**) and plywood cladding system (**c**).

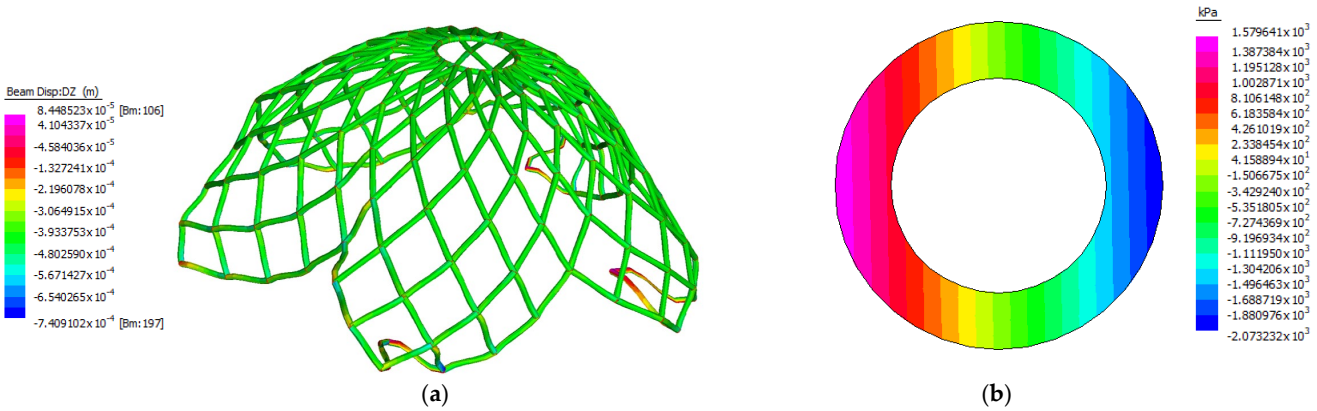

Figure 19. Strand7 analysis of Case Study One—Iteration One showing the maximum fiber stresses of bamboo beams of the combined structural system showing the deformed shape (**a**) and fiber stresses by cross-sectional area (**b**).

When considering the ultimate stress capacity of bamboo, the structure is significantly rigid, especially towards the apex of the roof. This could be due to the spacing between bamboo members, as defined by the grid spacing, which allows the structure to sustain

more lateral and gravity loads. A short comparison of the design stresses with the ultimate stress capacity is shown in Table 7.

Table 7. Tensile and compressive fiber stresses for Case Study One—Iteration One.

	Tension Stress	Compression Stress
Failure Stresses (kPa)	43,500	43,500
Design Stresses (kPa)	1580	2073
Utilized Ratio	3.6%	4.8%

3.7.2. Analysis of Iteration Two of Lotus Shelter

The deformed shapes of the second iteration show a similar concentrated stress at the base connections to the ground and the highest point of each opening. However, as shown in Figure 20, due to the change in grid spacing and bamboo, the bamboo beams appear to experience more of the loading compared to the plywood cladding. Figure 21 shows the fiber stresses along the cross-sectional area, experiencing a maximum tensile force of 12,030 kPa and a maximum compressive force of 11,810 kPa. A summary of these forces is shown in Table 8.

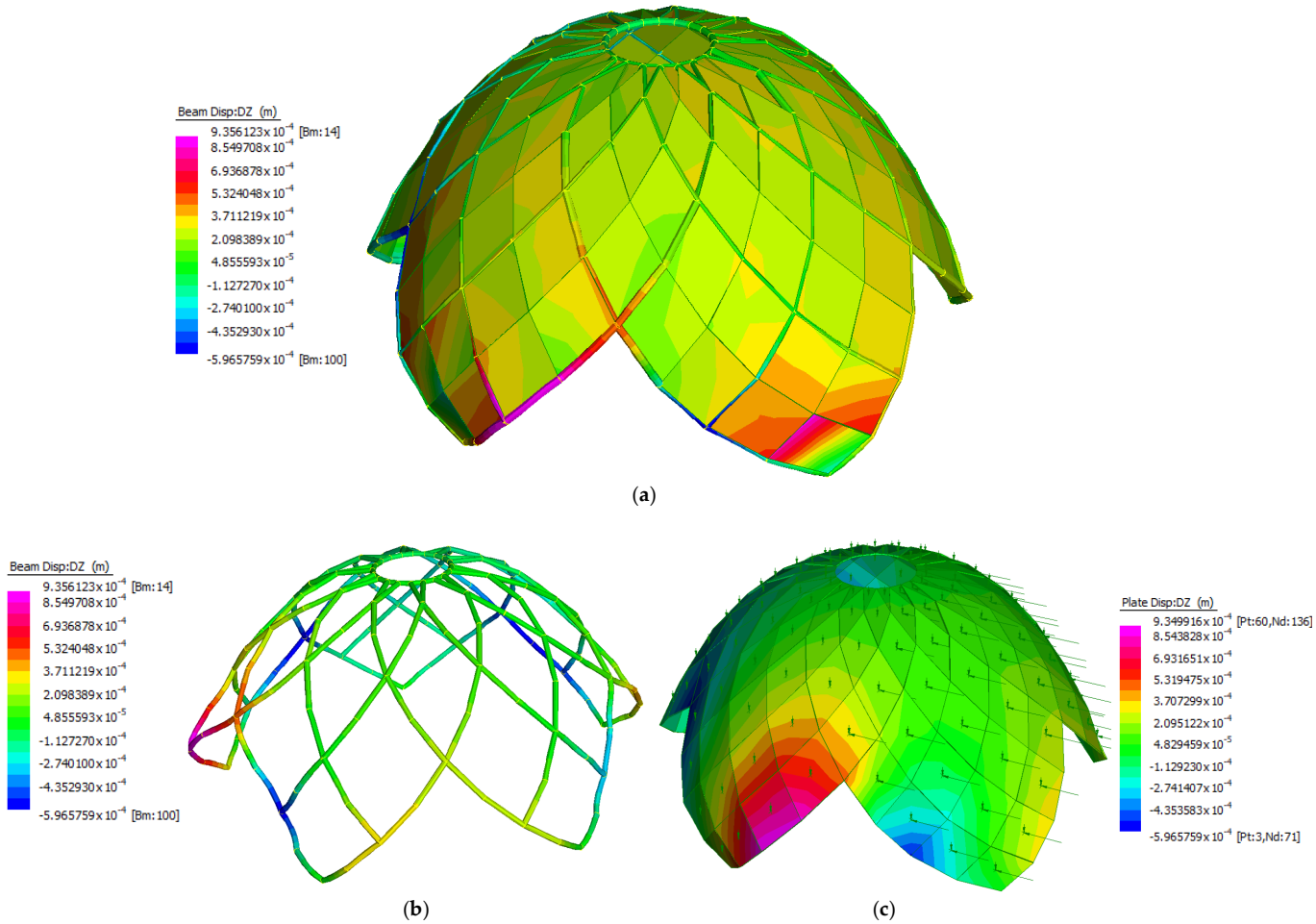

Figure 20. Strand7 analysis of Case Study One—Iteration Two showing the deformed shape of the combined structural system (**a**). An isolated analysis was conducted for the structural beams (**b**) and plywood cladding system (**c**).

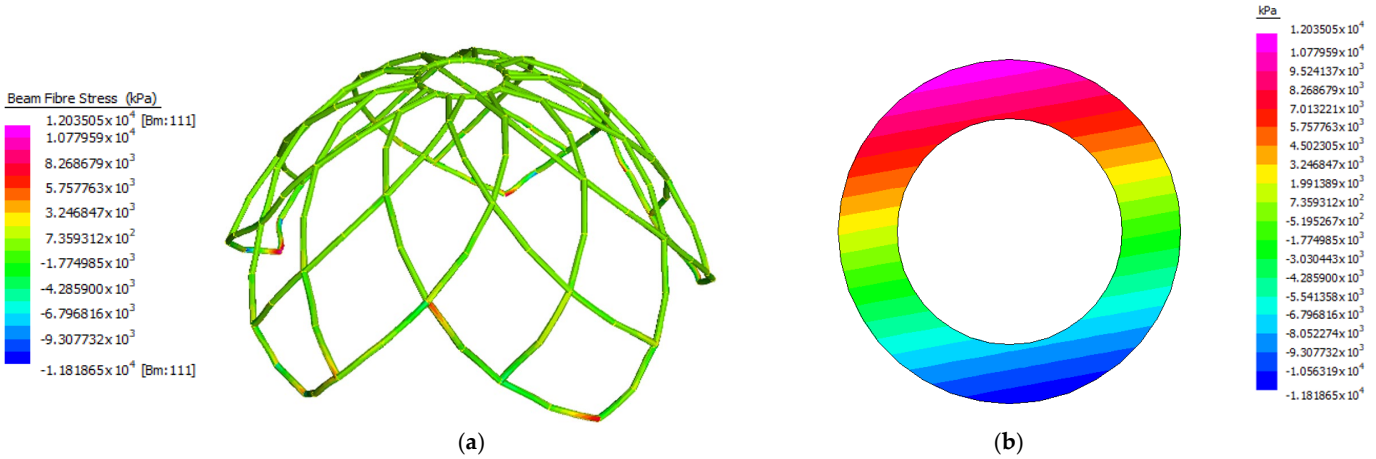

(**a**) (**b**)

Figure 21. Strand7 analysis of Case Study One—Iteration Two showing the maximum fiber stresses of bamboo beams of the combined structural system showing the deformed shape (**a**) and fiber stresses by cross-sectional area (**b**).

Table 8. Tensile and compressive fiber stresses for Case Study One—Iteration Two.

	Tension Stress	**Compression Stress**
Failure Stresses (kPa)	43,500	43,500
Design Stresses (kPa)	12,030	11,810
Utilization Ratio	27.7%	27.1%

3.7.3. Analysis of Iteration Three of Lotus Shelter

The deflections are double those in the second design iteration; however, they are still within the acceptable range. The deformed shapes of the final iteration show a similar concentrated stress around the openings of the shelter. As shown in Figure 22, the bamboo beams continue to experience more of the loading compared to the plywood cladding. Figure 23 shows the fiber stresses along the cross-sectional area, experiencing a maximum tensile force of 19,006 kPa and a maximum compressive force of 19,600 kPa. When similarly compared to the ultimate stress capacity of bamboo, the utilization is significantly larger than previous iterations. A short comparison of the design stresses with the ultimate stress capacity is shown in Table 9. It was noted that the plate and beam displacement were the same in the analysis for this iteration.

Table 9. Tensile and compressive fiber stresses for Case Study One—Iteration Three.

	Tension Stress	**Compression Stress**
Failure Stresses (kPa)	43,500	43,500
Design Stresses (kPa)	19,006	19,600
Utilized Ratio	43.7%	45.5%

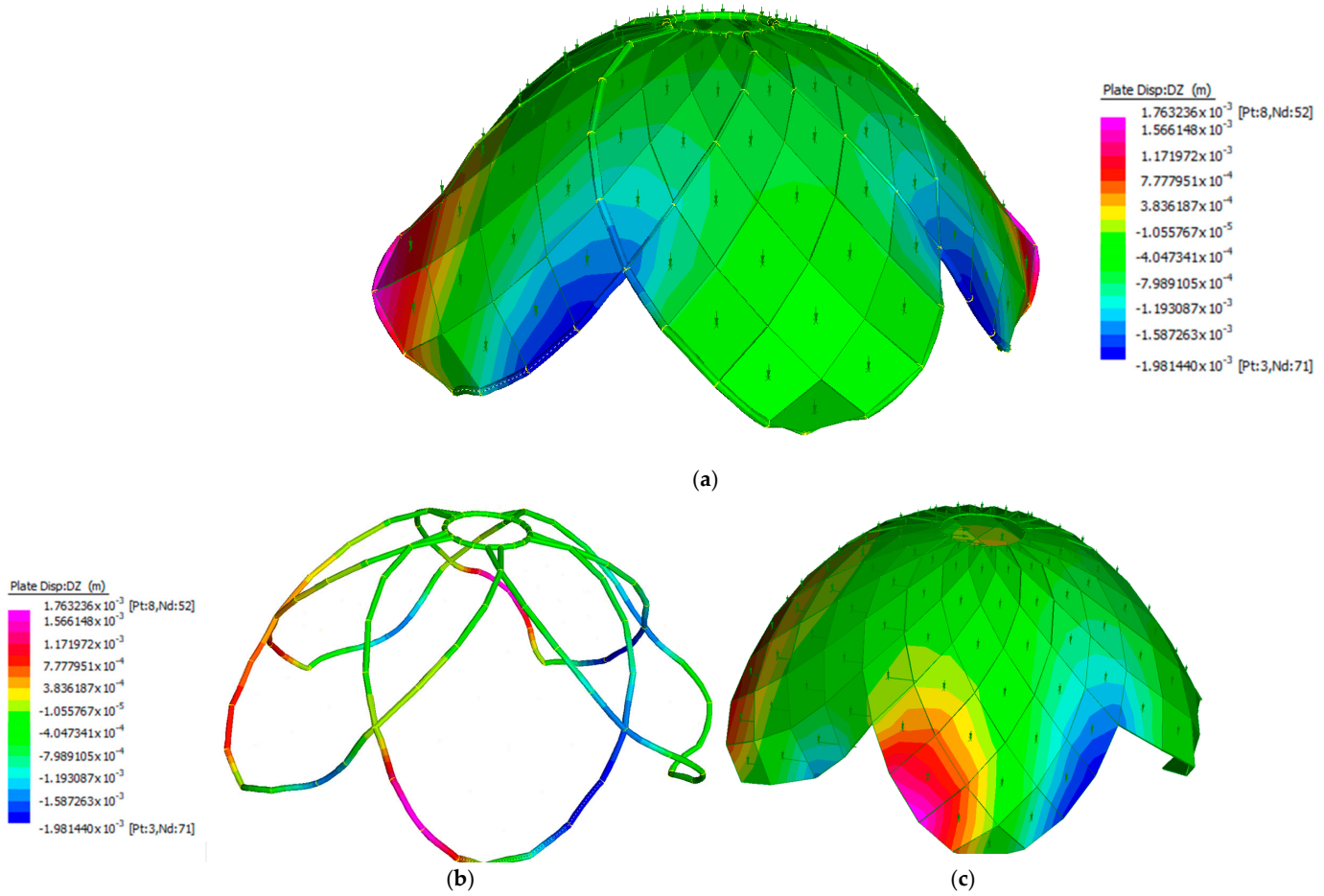

Figure 22. Strand7 analysis of Case Study One—Iteration Three showing the deformed shape of the combined structural system (**a**). An isolated analysis was conducted for the structural beams (**b**) and plywood cladding system (**c**).

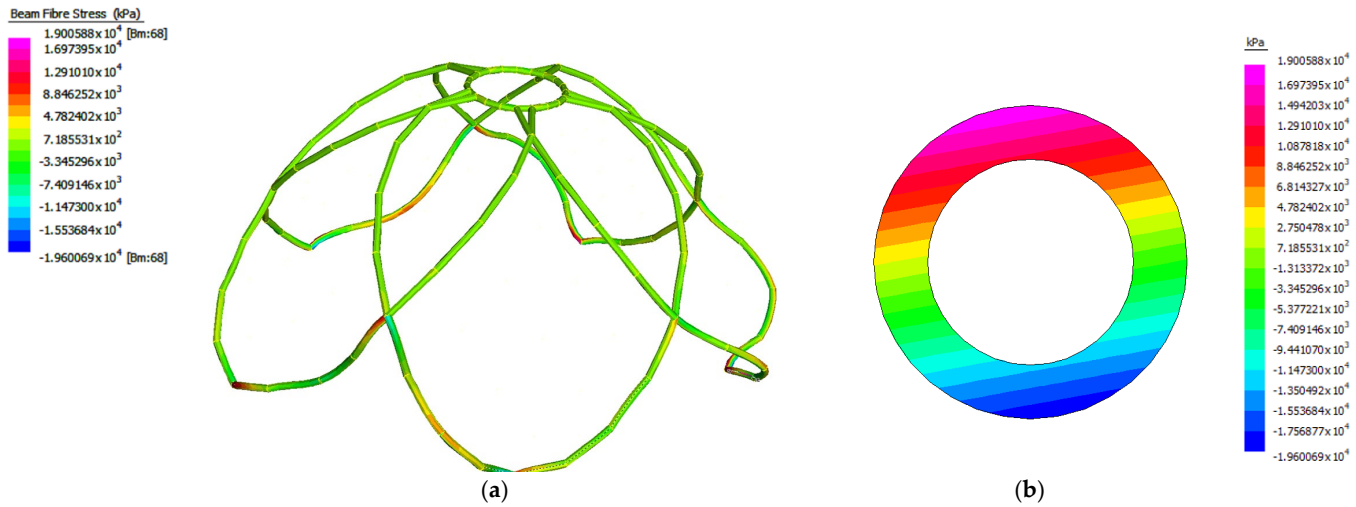

Figure 23. Strand7 analysis of Case Study One—Iteration Three showing the maximum fiber stresses of bamboo beams of the combined structural system showing the deformed shape (**a**) and fiber stresses by cross-sectional area (**b**).

3.7.4. Additional Analysis for Case Study One

Using Design Iteration Three, an additional investigation into the role of the plywood cladding was conducted to assess the magnitude of deflections. As previous iterations used the plywood cladding as a finishing or outer membrane, the conducted analysis below observes the differences when the cladding is placed between the bamboo members, increasing their lateral stability. As shown in the above figures, the deflection is reduced by a factor of 5.8 according to the ratio of displacement.

$$Ratio = \left(1.378 \times 10^{-3}\right) / \left(2.38 \times 10^{-4}\right) = 5.8 \quad (7)$$

As shown in Figure 24, the plywood cladding further contribute to reducing the load distribution throughout the structure. While the forces are distributed through the bamboo stems, the cladding provides additional lateral resistance that controls a large magnitude of the torsional stresses and deflections. Figure 24a shows the deformed shape (at a 5% exaggeration mode on Strand7) without the cladding, highlighting the significant difference. The bamboo stems experience a larger magnitude of beam stresses at the base of the structure at a maximum of 1.378 mm, particularly at the apex (in dark blue) around the openings. As shown in Figure 24b, the loads are redistributed to the base connections, reducing the loading at the apex.

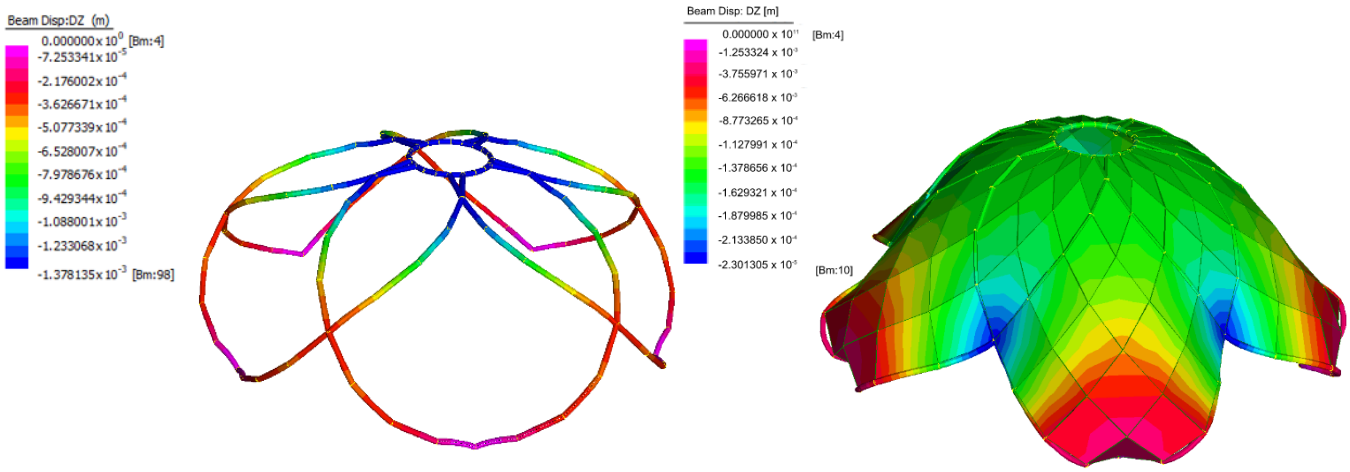

(**a**) (**b**)

Figure 24. Additional Strand7 Analysis of deflection of bamboo beams system showing the deformed shape (**a**) compared to the combined cladding and beams structural system (**b**).

3.8. Static Load Analysis for Case Study Two—Modular Community Pavilion

3.8.1. Analysis of Iteration One of Modular Community Pavilion

Figure 25 shows the largest deflection mode of the design due to the load combination, G + 0.7Q + W. This presents a weakness around the perimeter of the apex. Furthermore, the design is shown to exceed the Fiber Stress Limit, previously specified in Table 6, with a maximum stress of 65.1 MPa, 49.7% larger than the limit. A short comparison of the design stresses with the ultimate stress capacity is shown in Table 10.

Table 10. Tensile and Compressive fiber stresses for Case Study Two—Iteration One.

	Tension Stress	**Compression Stress**
Failure Stresses (kPa)	43,500	43,500
Design Stresses (kPa)	42,201	65,106
Utilization Ratio	97%	150%

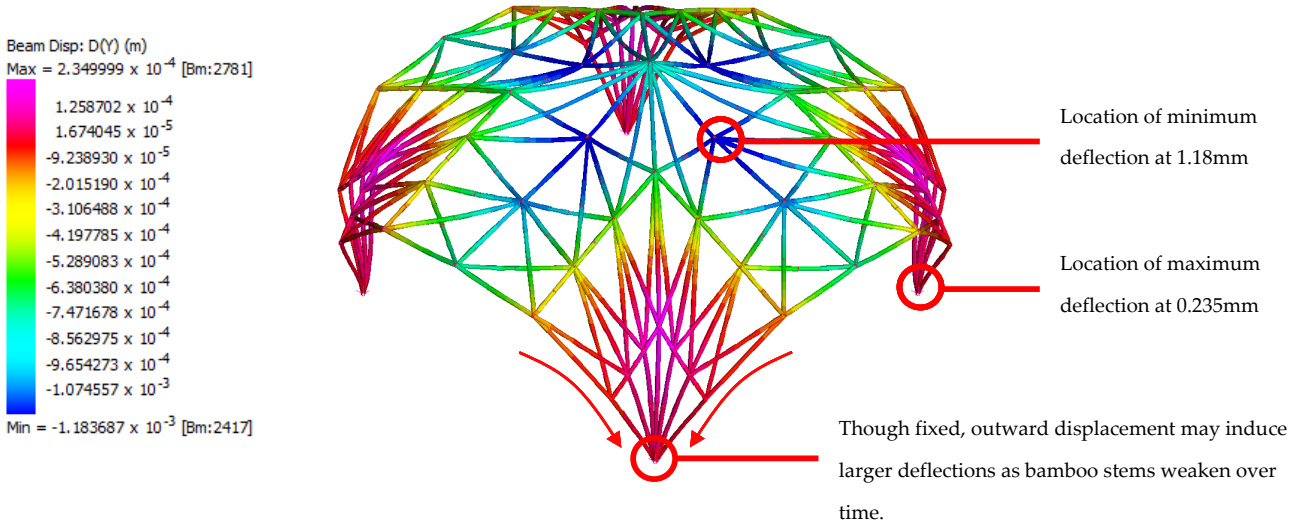

Figure 25. Strand7 analysis of Case Study Two—Iteration One showing the most critical deformed shape of the combined structural system, under load case G + 0.7Q + W.

The location of the extreme deflections correlates with the fibre stresses, whereby, the highest magnitudes of the stresses are concentrated at the apex and the base connections. This can be observed to be distributed from the mid-span of the pavilion's openings. As indicated in Figure 26, the unsupported bamboo beams experience a larger fibre stress and sagging bending moment, due to the grid-spacing between primary members at 1.5 m. This is observed across all elevations of the pavilion, due to its symmetry.

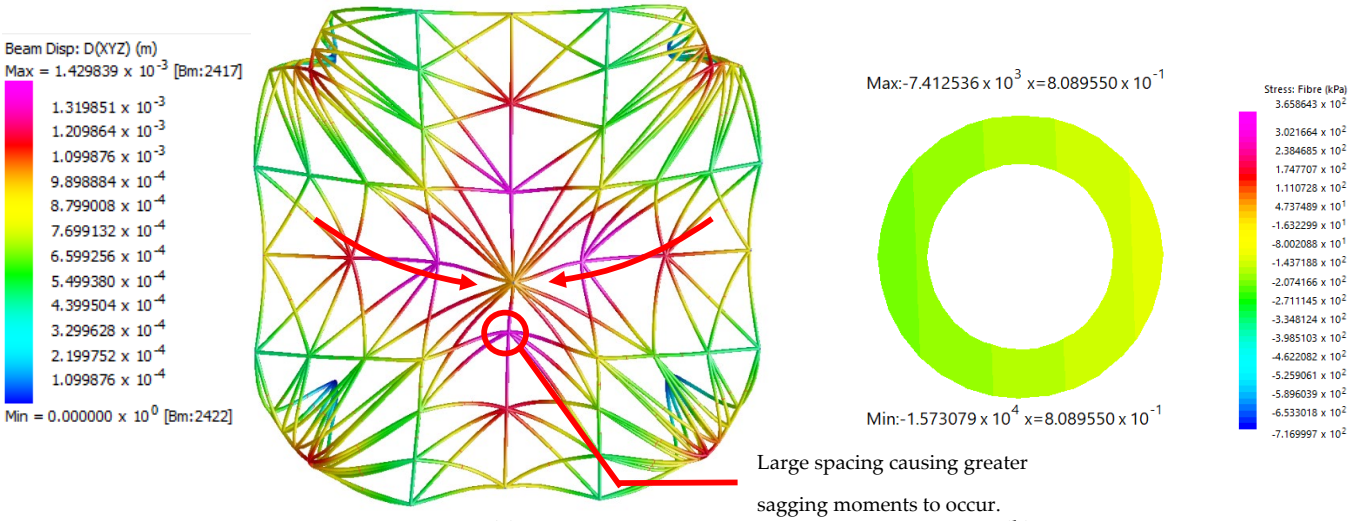

Figure 26. Strand7 analysis of Case Study Two—Iteration One showing the maximum fiber stresses of bamboo beams of the combined structural system showing the deformed shape under wind load (**a**) and fiber stresses by cross-sectional area (**b**).

3.8.2. Analysis of Iteration Two of Modular Community Pavilion

Figure 27 shows the largest deflection mode of the design at 10% due to the load combination, 1.2G +1.5Q. This demonstrates a significant improvement in the deflection when compared to the previous iteration. Though there is a similar weakness at the apex, the magnitude of the deflection is reduced by almost 50%. This could be due to the improved continuity between the secondary members, which better distributes the magnitude of the loads to the base supports.

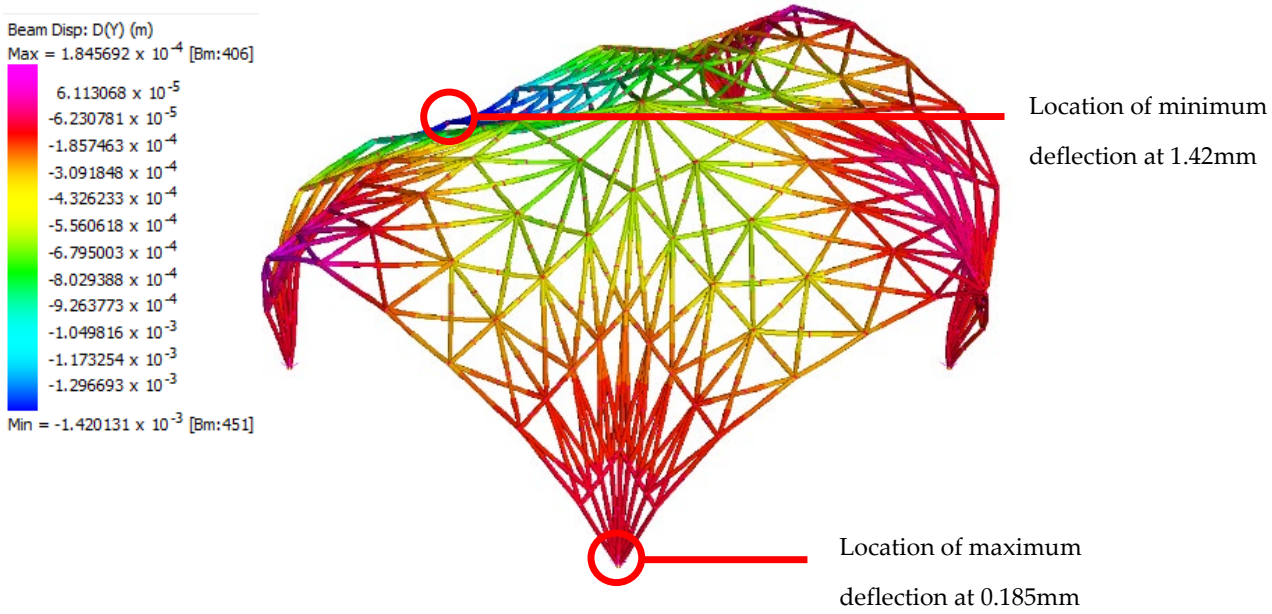

Figure 27. Strand7 analysis of Case Study Two—Iteration Two showing the most critical deformed shape of the combined structural system, under load case 1.2G + 1.5Q.

This shows an even distribution of the loading conditions with no significant pressures, when compared to the initial design. Due to the shorter grid-spacing of 1.2 m, the loads are shown to be more evenly distributed, reducing concentrated areas of deflections. This is similar to the fiber stresses, as shown in Figure 28. bending moment is greatly reduced. The maximum compressive stress is 213 MPa and the maximum tensile stress is 437 MPa. A short comparison of the design stresses with the ultimate stress capacity is shown in Table 11.

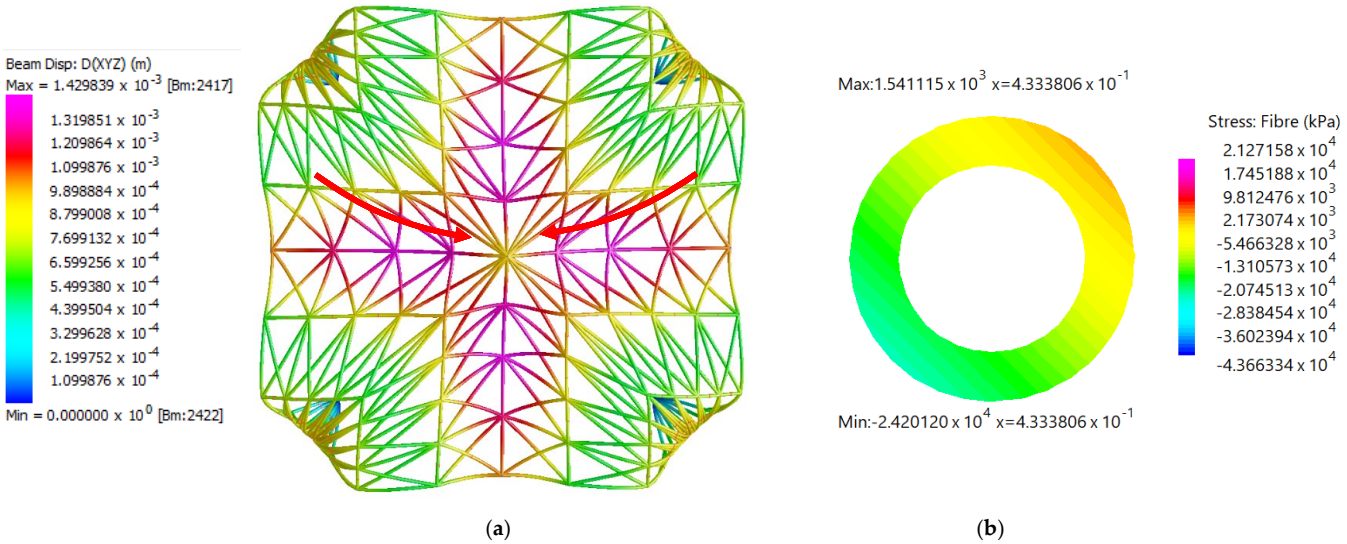

(**a**) (**b**)

Figure 28. Strand7 analysis of Case Study Two—Iteration Two showing the maximum fiber stresses of bamboo beams of the combined structural system showing the deformed shape under wind load (**a**) and fiber stresses by cross-sectional area (**b**).

Table 11. Tensile and compressive fiber stresses for Case Study Two—Iteration One.

	Tension Stress	Compression Stress
Failure Stresses (kPa)	43,500	43,500
Design Stresses (kPa)	21,272	43,663
Utilization Ratio	49%	100%

3.8.3. Analysis of Iteration Three of Modular Community Pavilion

Figure 29 shows a similar result to the previous iteration. The most critical loading combination being found to be 1.2G + W + Q, whereby a maximum deflection of 1.71 mm and minimum deflection of 0.117 mm was observed. While the Strand7 Analysis demonstrates that the deflections are distributed across the pavilion, the lower magnitude in the deflections indicate the efficiency of structure in comparison to its previous iterations. Thus, the increase in additional members allows for a greater balance between the tensile and compressive forces with the 0.8 m grid spacing. This is further supported by the apparent symmetry of the design.

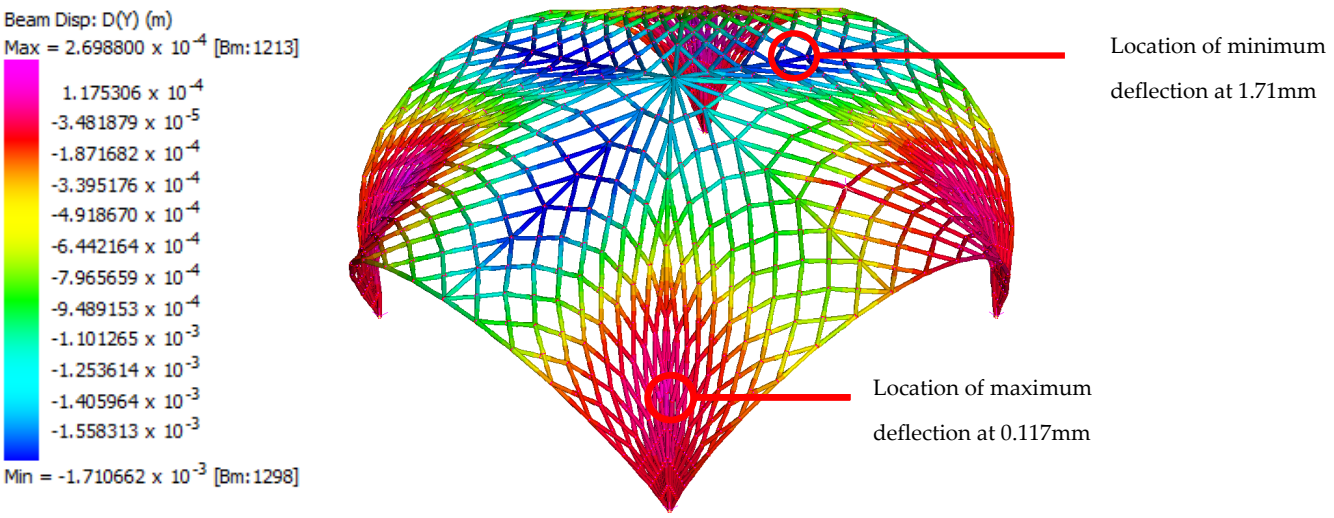

Figure 29. Strand7 analysis of Case Study Two—Iteration Three showing the most critical deformed shape of the combined structural system, under load case 1.2G + W + Q.

This is also observed in the distribution of the wind pressures throughout the structures as shown in Figure 30, whereby the displacements due to the wind loads correlate with the deflections shown above. The maximum compressive stress is 245 MPa and the maximum tensile stress is 211 MPa. A short comparison of the tensile and compressive stresses across all three iterations with the ultimate stress capacity is shown in Table 12.

Table 12. Tensile and compressive fiber stresses for Case Study Two—Iteration One.

	Tension Stress	Compression Stress
Failure Stresses (kPa)	43,500	43,500
Design Stresses (kPa)	245	211
Utilization Ratio	0.56%	0.49%

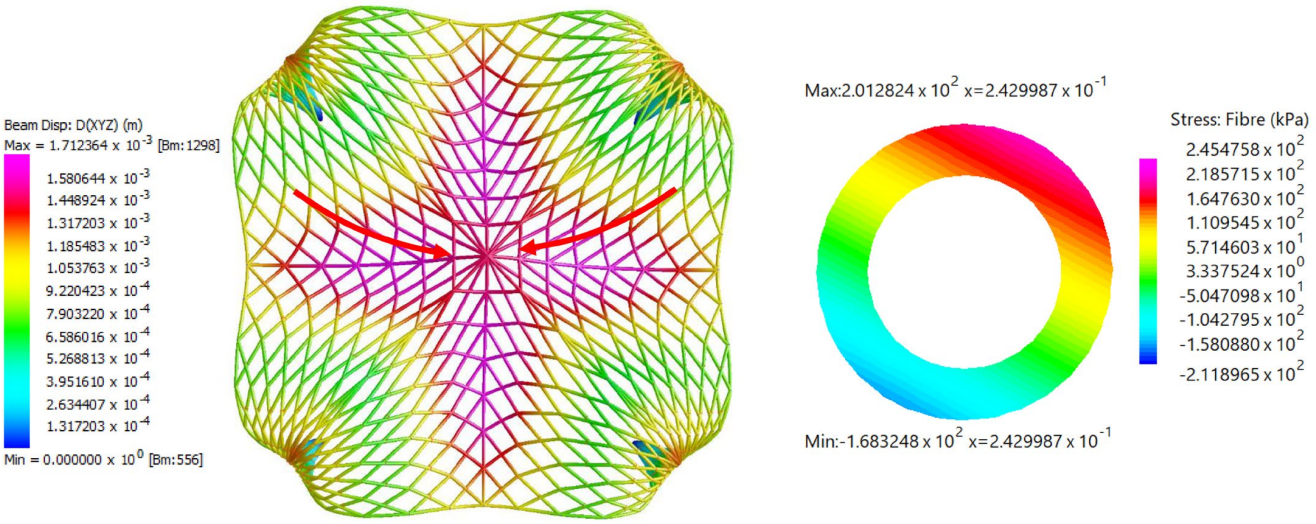

(**a**) (**b**)

Figure 30. Strand7 analysis of Case Study Two—Iteration Three showing the maximum fiber stresses of bamboo beams of the combined structural system showing the deformed shape under wind load (**a**) and fiber stresses by cross-sectional area (**b**).

4. Results

4.1. Structural Analysis of Buddhist Lotus Shelter

A comparison between the displacements, axial stress, and fiber stresses was conducted. The grid size was a significant factor in addressing the behaviors of each design. However, the deflection and fiber stresses were still significantly lower that the limits specified in the design criteria.

4.1.1. Displacement Analysis

As discussed in Section 3.5, the displacement of each design was significantly lower than the deflection limit. Figure 31 presents a comparison of the deflections for each design, whereby Iteration Three shows the largest deflections. The full results of this analysis are detailed in Appendix A, Table A2.

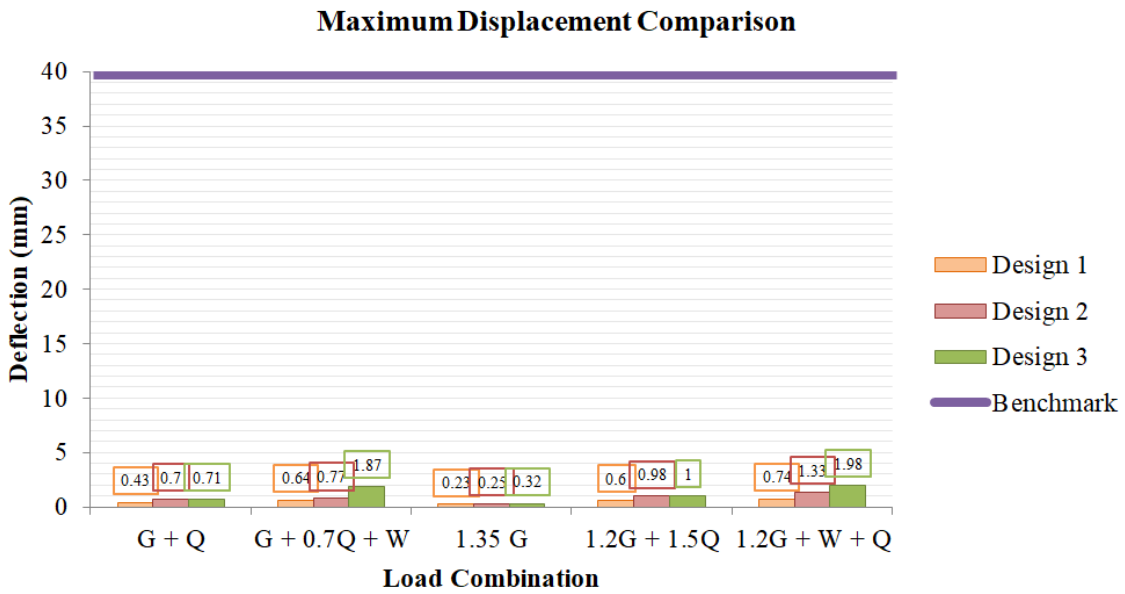

Figure 31. Comparison of deflections (along the z-direction) between each design.

4.1.2. Fiber Stress Analysis

Figure 32 compares the maximum fiber stresses of each design. Iteration Three is shown to experience the largest magnitude of fiber stresses, particularly in the cases of 1.35G and 1.2G + W + Q. This could be attributed to the reduction in the number of bamboo stems increasing the amount of load that is sustained by the stems. The full results of this analysis are detailed in Appendix A, Table A3.

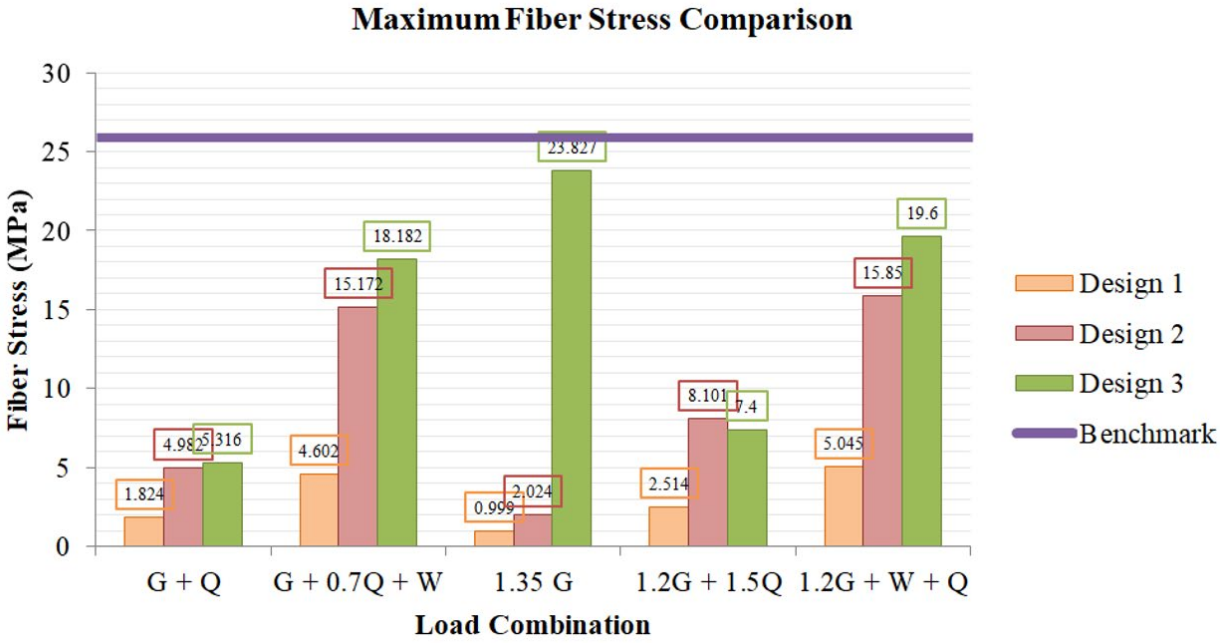

Figure 32. Comparison of fiber stresses (along the y-direction) of each design.

4.1.3. Summative Evaluation of Key Findings—Case Study One

Based on the previous findings, all three iterations of the first case study satisfied the design criteria stated in Section 3.2 by a significant margin. The use of the structural form has most likely contributed to the integrity of the design, whereby the symmetry and interlocking bamboo stems facilitated an even load distribution throughout. As the first case study considered rotational symmetry, the design had an increased lateral stability, which reduced the magnitude of displacement regardless of grid size. Furthermore, the inclusion of plywood cladding further supported the structure, reducing the wind effects even further. This can be observed between the first and the second iteration.

4.2. Structural Analysis of Modular Community Pavilion

4.2.1. Displacement Analysis

Figure 33 shows a comparison between the deflections of each design, highlighting that the most significant is the Ultimate Limit State Combination—1.2G + 1.5Q—especially for Iteration One. All designs were well below the deflection limit of 26.15 mm, which validates the structural scheme in all cases. However, Iteration One shows significantly larger displacements, which could cause prolonged damage over time due to bending stresses. The full results of this analysis are detailed in Appendix B, Table A4.

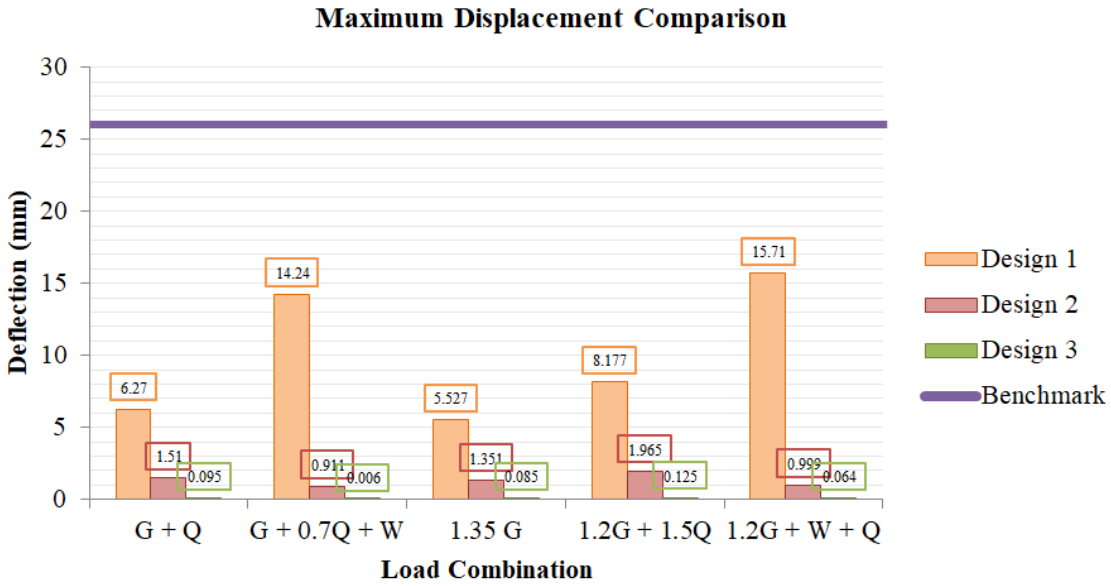

Figure 33. Comparison of deflections (along the z-direction) between each design.

4.2.2. Axial Stress Analysis

Figure 34 presents a comparison of the compressive axial stress along the Z axis, as bamboo is much weaker under compression due to its composition as a fibrous material and the sectional capacity of each stem. All designs show axial stresses well below the tensile capacity of Natural Bamboo of 108 MPa. Iteration Two appears to experience greater axial stress, which may be a modeling error. As the benchmark is beyond the results, it was not included in the graph. The full results of this analysis are detailed in Appendix B, Table A5.

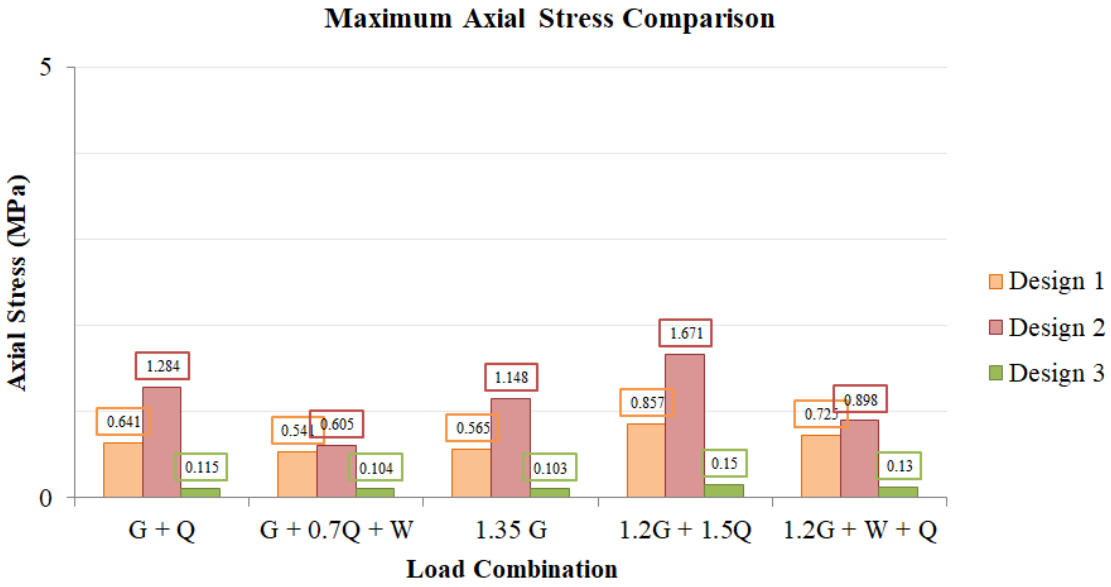

Figure 34. Comparison of axial stresses (along the z-direction) between each design.

4.2.3. Fiber Stress Analysis

Figure 35 presents a comparison of fiber stresses experienced along the xx plane. While Iteration One and Three are within the stress limit of 43.5 MPa, Iteration One greatly exceeds this under the load combination of 1.2G + 1.5Q, which indicates that the gravity loads are the most critical for this design. Iteration Three shows considerably low stresses

in all cases, which may be attributed to the design connections and the repetition of the grid shell across a smaller area. The full results of this analysis are detailed in Appendix B, Table A6.

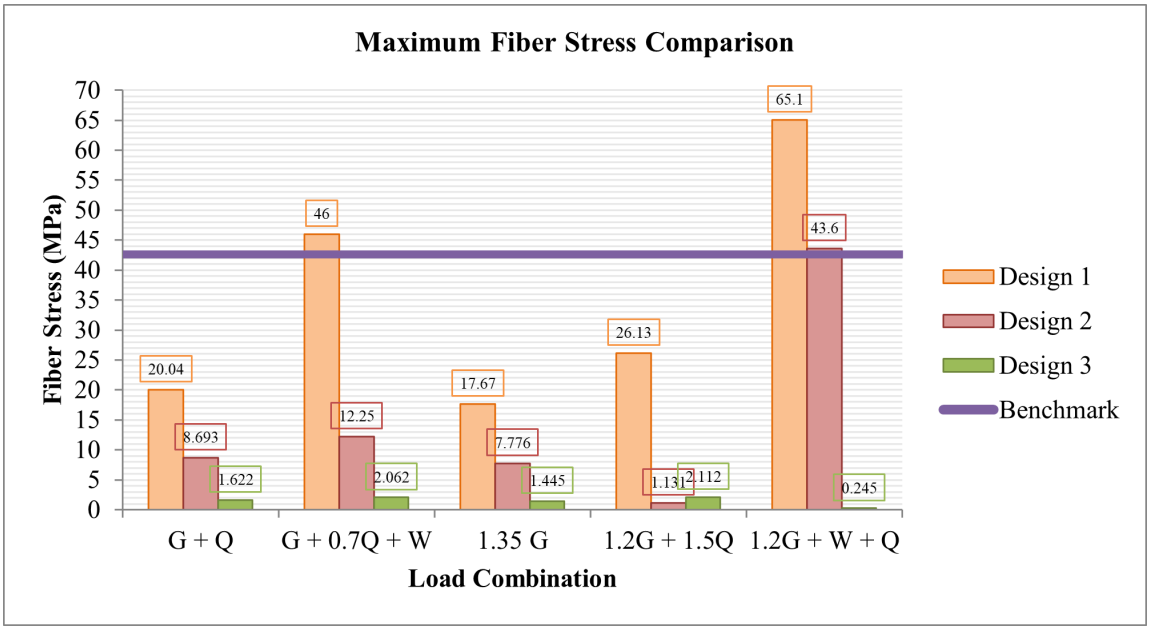

Figure 35. Comparison of fiber stresses (along the y-direction) between each design.

4.2.4. Evaluation of Key Findings—Case Study Two

Similarly for the second case study, all three iterations mostly satisfied the design criteria stated in Section 3.3 by a significant margin. As the initial design considered bilateral symmetry, there was an even distribution of loads throughout the structure. The most notable difference between each iteration is the magnitude of the fiber stresses. In contrast to the first case study, each design did not include cladding, resulting in increased fiber stresses. However, the results reflect that the increase in grid size does, in fact, increase the rigidity of the design, allowing the design to sustain larger static loads throughout. The end supports experienced the magnitude of gravity loads, particularly due to the wind loading. However, an assessment of the dynamic loading is out of the scope of this study.

5. Conclusions

This paper presented different architectural case studies of preliminary grid-shell structures that explore the structural capacity and adaptability of bamboo. As examples of complex structural scenarios modeled in Rhino with Grasshopper, three iterations of each design were assessed under static loading conditions, using finite element analysis in Strand7, to highlight the structural behavior of natural bamboo over low-rise and long-spanning designs. The results show that the rigidity and strength of the bamboo was governed by the repetition and symmetry of the two typologies, which increased their lateral stability and the distribution of static loads throughout the design. The flexibility of bamboo in facilitating the curvature of multiple design components contributed to a harmonious structural system that resisted large displacements and reduced individualized stresses on each structural member.

This structural study also provides preliminary insight into the value of bamboo as a low-carbon material and emphasizes opportunities to experiment with the variability of mechanical properties between bamboo species through modeling. Assessing the structural behavior of bamboo using complex architectural contexts can help in testing various design strategies, including concrete base supports and interlocking fixed connections, to standardize its mechanical performance. The novelty of this study is in its encouraging the

use of architectural modeling to assess the structural behavior of complex structures and the effect of materials on overall performance.

Author Contributions: Conceptualization, F.T., W.Z. and B.M.; Methodology, F.T., W.Z. and B.M.; Software, F.T., W.Z. and B.M.; Validation, F.T., W.Z. and B.M.; Formal analysis, F.T., W.Z. and B.M.; Investigation, F.T., W.Z. and B.M.; Resources, F.T. and K.S.; Data curation, W.Z., B.M. and K.S.; Writing—original draft, F.T, W.Z. and B.M.; Writing—review & editing, F.T. and K.S.; Supervision, K.S.; Project administration, K.S. All authors have read and agreed to the published version of the manuscript.

Funding: This research received no external funding.

Institutional Review Board Statement: Not applicable.

Informed Consent Statement: Not applicable.

Data Availability Statement: The raw data supporting the conclusions of this article will be made available by the author (Faham Tahmasebinia) on request.

Conflicts of Interest: The authors declare no conflicts of interest.

Appendix A

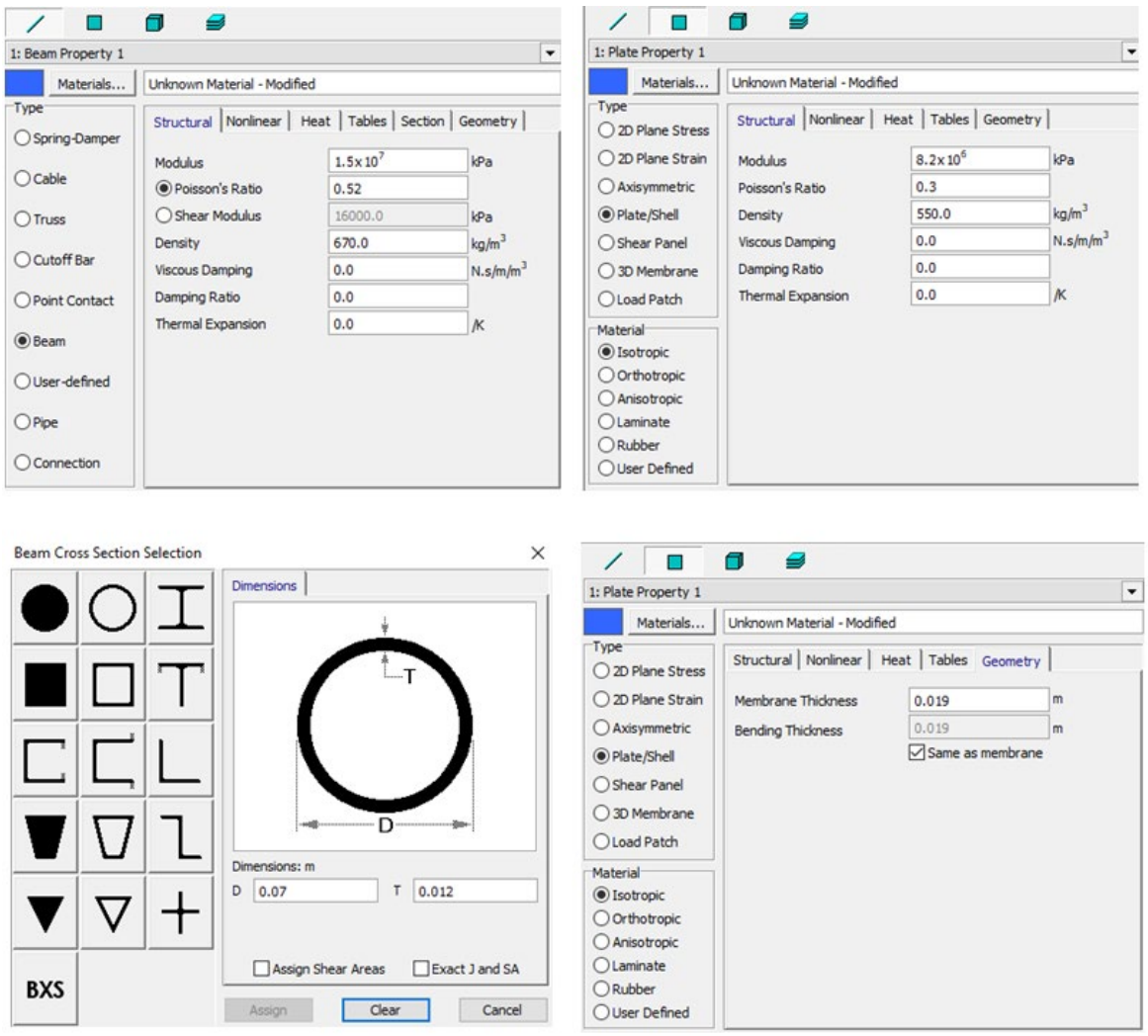

Figure A1. Inserted properties of beams and plates for Buddhist Lotus Shelter analysis.

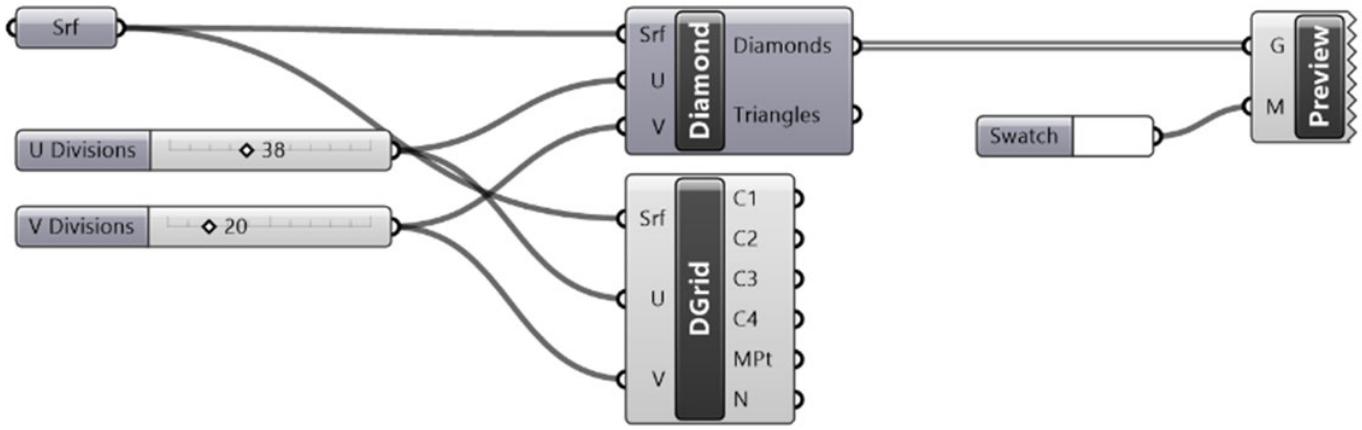

Figure A2. Grasshopper code for Lotus Dome shape.

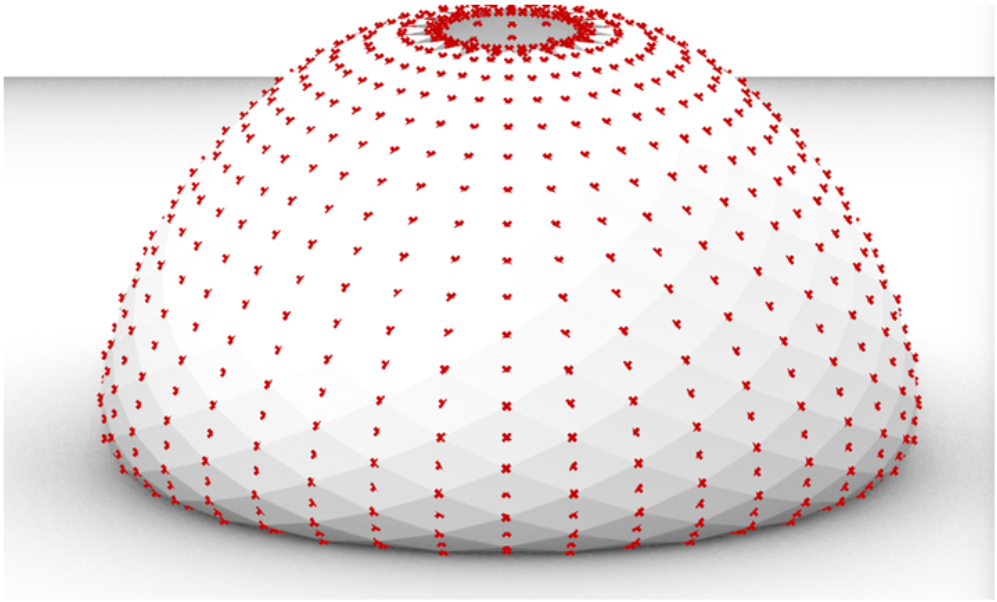

Figure A3. Construction of Dome using Grasshopper and Rhino.

Table A1. Tabulated Results of Iteration of Buddhist Lotus Shelter.

Iteration/Load Case	Design 1	Design 2	Design 3
Grid (m)	0.6	1.2	2.4

Table A2. Maximum displacement (mm)—critical case is **bolded**.

Iteration/Load Case	G + Q	G + 0.7Q + W	1.35 G	1.2G + 1.5Q	1.2G + W + Q
Design 1	0.43	0.64	0.23	0.6	**0.74**
Design 2	0.7	0.77	0.25	**0.98**	1.33
Design 3	0.71	1.87	0.32	1	**1.98**

Table A3. Maximum fiber stresses (MPa).

Iteration/Load Case	G + Q	G + 0.7Q + W	1.35 G	1.2G + 1.5Q	1.2G + W + Q
Design 1	1.824	4.602	0.999	2.514	5.045
Design 2	4.982	15.172	2.024	8.101	15.85
Design 3	5.316	18.182	23.827	7.4	19.6

Appendix B

Appendix B.1. Tabulated Results of Iteration of Modular Community Shelter

Table A4. Maximum displacement (mm)—critical case is **bolded**.

Iteration/Load Case	G + Q	G + 0.7Q + W	1.35 G	1.2G + 1.5Q	1.2G + W + Q
Design 1	6.270	**14.24**	5.527	8.177	15.71
Design 2	1.510	0.911	1.351	**1.965**	0.999
Design 3	0.095	0.006	0.085	**0.125**	0.064

Table A5. Maximum axial stresses (MPa).

Iteration/Load Case	G + Q	G + 0.7Q + W	1.35 G	1.2G + 1.5Q	1.2G + W + Q
Design 1	0.641	0.541	0.565	0.857	0.725
Design 2	1.284	0.605	1.148	1.671	0.898
Design 3	0.115	0.104	0.103	0.150	0.130

Table A6. Maximum fiber stresses (MPa)—critical case is **bolded**.

Iteration/Load Case	G + Q	G + 0.7Q + W	1.35 G	1.2G + 1.5Q	1.2G + W + Q
Design 1	20.04	46.00	17.67	26.13	**65.1**
Design 2	8.693	**12.25**	7.776	1.131	43.1
Design 3	1.622	2.062	1.445	**2.112**	0.245

Appendix B.2. Summary of Applied Loads on Members (kPa) Rough Calculations

Table A7. Calculated uniformly distributed loads for G, Q, and W (Load x Tributary Width).

Iteration/Case	Dead Load	G	Live Load	Q	Wind Load	W
Design 1 Trib. Width = 1.7 (m)	0.47	0.8	0.25	0.43	1	1.7
Design 2 Trib. Width = 1.2 (m)	0.47	0.56	0.25	0.3	1	1.2
Design 3 Trib. Width = 0.7 (m)	0.47	0.33	0.25	0.175	1	0.7

Appendix B.3. Showcase of Initial Grasshopper Code for Modular Community Shelter

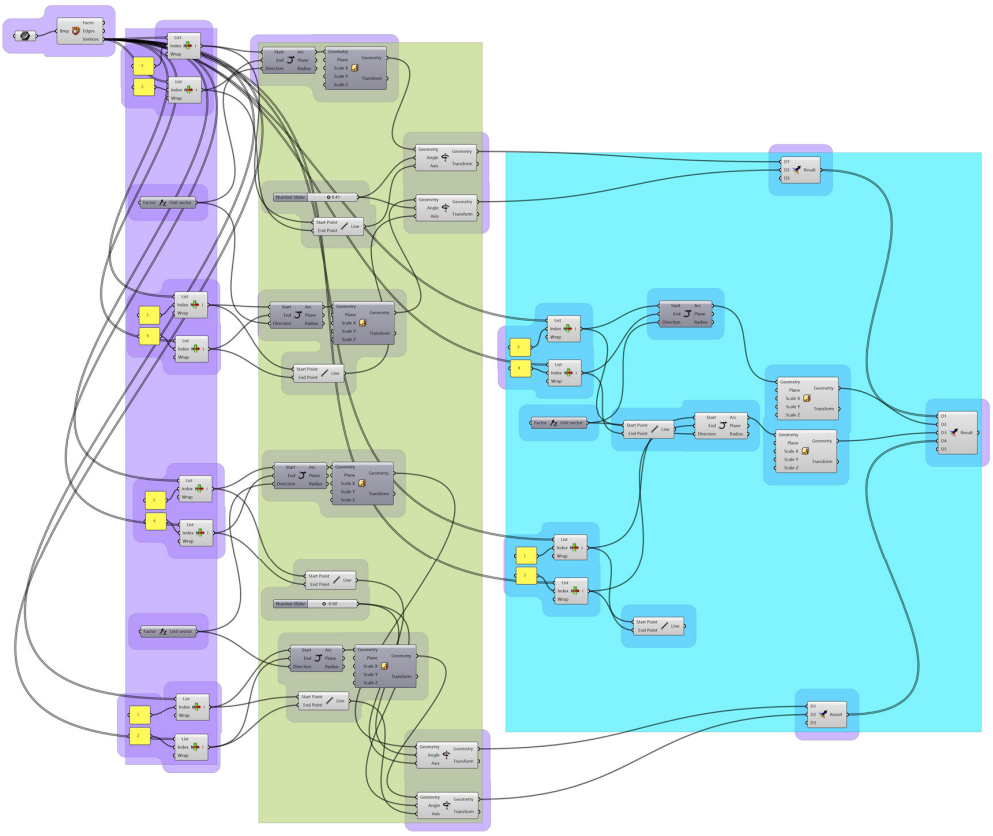

(**a**)

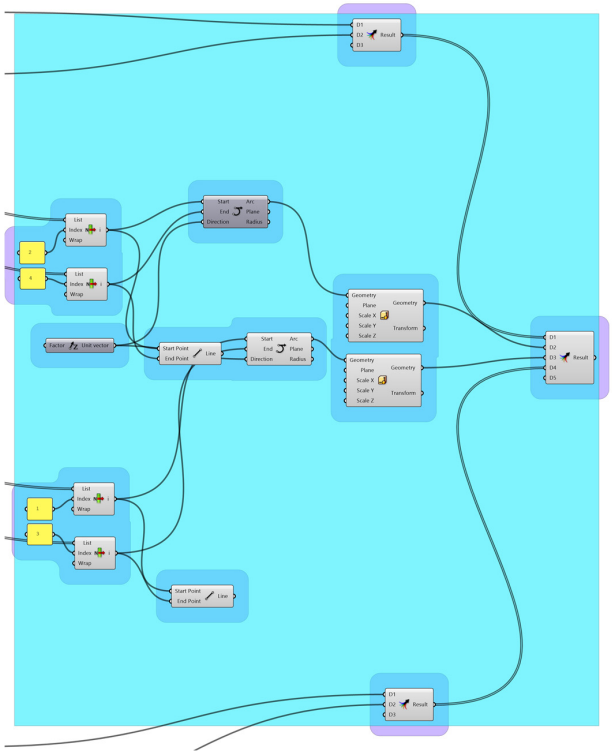

(**b**)

Figure A4. Grasshopper code for building form by first establishing the plane and forming the base frame (**a**), then implementing the circular hollow section and material (**b**).

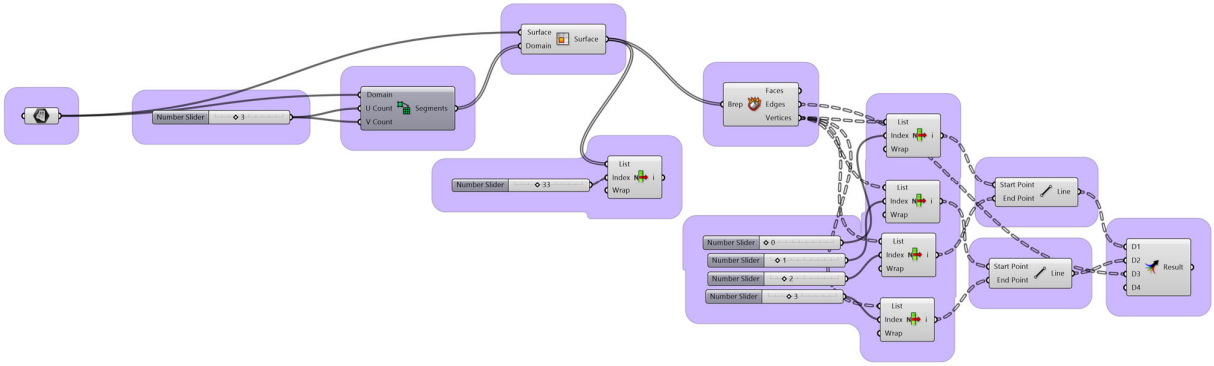

(**a**)

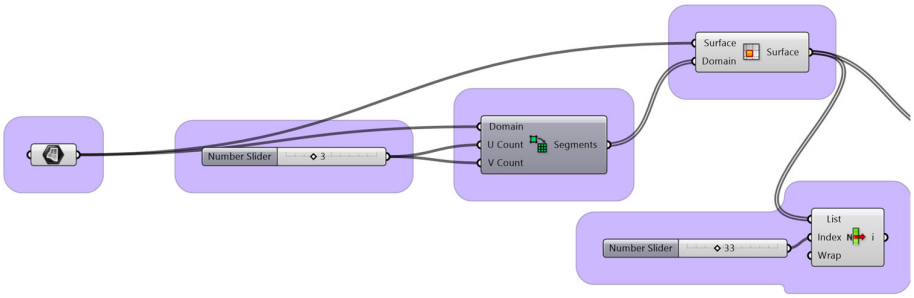

(**b**)

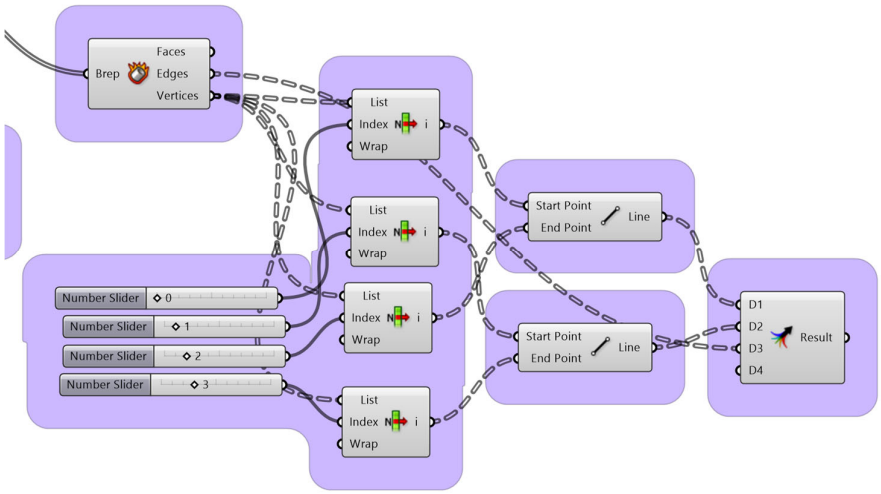

(**c**)

Figure A5. Grasshopper code for lattice structure to support design form for Modular Community Pavilions, showing full Grasshopper code (**a**), and broken down by span (**b**,**c**).

References

1. Chan, M.; Masrom, A.N.; Yasin, S.S. Selection of Low-Carbon Building Materials in Construction Projects: Construction Professionals' Perspectives. *Buildings* **2022**, *12*, 486. [CrossRef]
2. Santamouris, M.; Vasilakopoulou, K. Present and future energy consumption of buildings: Challenges and opportunities towards decarbonisation. *E-Prime-Adv. Electr. Eng. Electron. Energy* **2021**, *1*, 100002. [CrossRef]
3. Minunno, R.; O'Grady, T.; Morrison, G.M.; Gruner, R.L. Investigating the embodied energy and carbon of buildings: A systematic literature review and meta-analysis of life cycle assessments. *Renew. Sustain. Energy Rev.* **2021**, *143*, 110935. [CrossRef]
4. Yiping, L.; Yanxia, L.; Buckingham, K.; Henley, G.; Guomo, Z. Bamboo and Climate Change Mitigation. INBAR Technical Reports. 2010. Available online: https://www.inbar.int/resources/inbar_publications/bamboo-and-climate-change-mitigation (accessed on 18 February 2024).
5. Xiao, Y. *Engineered Bamboo Structures*; CRC Press: London, UK, 2022. [CrossRef]
6. Chaowana, K.; Wisadsatorn, S.; Chaowana, P. Bamboo as a Sustainable Building Material—Culm Characteristics and Properties. *Sustainability* **2021**, *13*, 7376. [CrossRef]

7. Tahmasebinia, F.; McDougall, R.; Sepasgozar, S.; Abberton, E.; Joung, G.H.; Joya, M.P.; Sepasgozar, S.M.E.; Marroquin, F.A. Development of Preliminary Curved Bamboo Member Design Guidelines through Finite Element Analysis. *Sustainability* **2020**, *12*, 822. [CrossRef]
8. Das, O.; Restás, Á.; Shanmugam, V.; Sas, G.; Försth, M.; Xu, Q.; Jiang, L.; Hedenqvist, M.S.; Ramakrishna, S. Demystifying Low-Carbon Materials. *Mater. Circ. Econ.* **2021**, *3*, 26. [CrossRef]
9. Sharma, B.; Gatóo, A.; Bock, M.; Ramage, M. Engineered bamboo for structural applications. *Constr. Build. Mater.* **2015**, *81*, 66–73. [CrossRef]
10. Correal, J.F. 14—Bamboo design and construction. In *Nonconventional and Vernacular Construction Materials*; Harries, K.A., Sharma, B., Eds.; Woodhead Publishing: Cambridge, UK, 2016; pp. 393–431. [CrossRef]
11. Wang, Y.; Yang, X.; Hou, Q.; Tao, J.; Dong, J. Quantitative Study on the Life-Cycle Carbon Emissions of a Nearly Zero Energy Building in the Severe Cold Zones of China. *Sustainability* **2022**, *14*, 1448. [CrossRef]
12. Global Status Report for Buildings and Construction. 2019. Available online: https://www.iea.org/reports/global-status-report-for-buildings-and-construction-2019 (accessed on 30 January 2024).
13. United Nations Environment Programme. *2022 Global Status Report for Buildings and Construction: Towards a Zero-Emission, Efficient and Resilient Buildings and Construction Sector*; United Nations Environment Programme: Nairobi, Kenya, 2022.
14. Grainger, A.; Smith, G. The role of low carbon and high carbon materials in carbon neutrality science and carbon economics. *Curr. Opin. Environ. Sustain.* **2021**, *49*, 164–189. [CrossRef]
15. Lapina, A.P.; I Zakieva, N. Bamboo in modern construction and architecture. *IOP Conf. Series Mater. Sci. Eng.* **2021**, *1083*, 012019. [CrossRef]
16. Minke, G. *Building with Bamboo: Design and Technology of a Sustainable Architecture*, 2nd ed.; Birkhäuser: Berlin, Germany; Boston, MA, USA, 2016. [CrossRef]
17. Dixon, P.G.; Gibson, L.J. The structure and mechanics of Moso bamboo material. *J. R. Soc. Interface* **2014**, *11*, 20140321. [CrossRef] [PubMed]
18. Wegst, U.G. Bending efficiency through property gradients in bamboo, palm, and wood-based composites. *J. Mech. Behav. Biomed. Mater.* **2011**, *4*, 744–755. [CrossRef] [PubMed]
19. Amada, S.; Untao, S. Fracture properties of bamboo. *Compos. Part B Eng.* **2001**, *32*, 451–459. [CrossRef]
20. Amada, S.; Ichikawa, Y.; Munekata, T.; Nagase, Y.; Shimizu, H. Fiber texture and mechanical graded structure of bamboo. *Compos. Part B Eng.* **1997**, *28*, 13–20. [CrossRef]
21. Nogata, F.; Takahashi, H. Intelligent functionally graded material: Bamboo. *Compos. Eng.* **1995**, *5*, 743–751. [CrossRef]
22. Shao, Z.-P.; Fang, C.-H.; Huang, S.-X.; Tian, G.-L. Tensile properties of Moso bamboo (Phyllostachys pubescens) and its components with respect to its fiber-reinforced composite structure. *Wood Sci. Technol.* **2010**, *44*, 655–666. [CrossRef]
23. Tahmasebinia, F.; Ma, Y.; Joshua, K.; Sepasgozar, S.; Yu, Y.; Li, J.; Sepasgozar, S.; Marroquin, F. Sustainable Architecture Creating Arches Using a Bamboo Grid Shell Structure: Numerical Analysis and Design. *Sustainability* **2021**, *13*, 2598. [CrossRef]
24. Thyrsostachys oliveri—Useful Tropical Plants'. Available online: https://tropical.theferns.info/viewtropical.php?id=Thyrsostachys+oliveri (accessed on 9 August 2023).
25. Zhang, Z.; Rao, F.; Wang, Y. Morphological, Chemical, and Physical–Mechanical Properties of a Clumping Bamboo (*Thyrsostachys oliveri*) for Construction Applications. *Polymers* **2022**, *14*, 3681. [CrossRef] [PubMed]
26. Banik, R.L. Morphology and Growth. In *Bamboo: The Plant and Its Uses*; Liese, W., Köhl, M., Eds.; Tropical Forestry; Springer International Publishing: Cham, Switzerland, 2015; pp. 43–89. [CrossRef]
27. Widyowijatnoko, A.; Harries, K.A. 20—Joints in bamboo construction. In *Nonconventional and Vernacular Construction Materials*, 2nd ed.; Harries, K.A., Sharma, B., Eds.; Woodhead Publishing Series in Civil and Structural Engineering; Woodhead Publishing: Cambridge, UK, 2020; pp. 561–596. [CrossRef]
28. Ma, C.Y.; Chan, Y.Y.J.; Crolla, K. Expanding bending-active bamboo gridshell streuctures' design solution space through hybrid assembly systems. In Proceedings of the 26th International Conference of the Association for Computer-Aided Architectural Design Research in Asia (CAADRIA) 2021, Hong Kong, China, 29 March–1 April 2021; Volume 1, pp. 331–340. [CrossRef]
29. A Buzalo, N.; O Versilov, S.; Platonova, I.D.; Tsaritova, N.G. Energy efficient building structures based on gridshell. *IOP Conf. Series Mater. Sci. Eng.* **2019**, *698*, 022010. [CrossRef]
30. Panyaden Bamboo Sports Hall. Bamboo Architecture', Bamboo Earth Architecture—Chiangmai Life Construction. Available online: https://www.bamboo-earth-architecture-construction.com/portfolio-item/panyaden-international-school-bamboo-sports-hall/ (accessed on 17 February 2024).
31. Green School Gymnasium—Atelier One'. Available online: https://www.atelierone.com/green-school-gymnasium/ (accessed on 17 February 2024).
32. Nocenco Cafe | VTN Architects—Arch2O.com. Available online: https://www.arch2o.com/nocenco-cafe-vtn-architects/ (accessed on 17 February 2024).
33. Lopez, D.S.; Stone, J.I. Two Buddhas Seated Side by Side: A Guide to the Lotus Sūtra'. In *Two Buddhas Seated Side by Side*; Princeton University Press: Princeton, NJ, USA, 2019; ISBN 0691189803.
34. *AS/NZS 1170.0:2002*; Structural Design Actions | SAI Global'. Standards New Zealand: Wellington, New Zealand, 2003. Available online: https://www.intertekinform.com/en-au/standards/ (accessed on 18 February 2024).

35. *AS/NZS 1170.2:2021*; Structural Design Actions, Part 2: Wind Actions. Standards New Zealand: Wellington, New Zealand, 2021. Available online: https://www.techstreet.com/standards/as-nzs-1170-2-2021?product_id=2229497 (accessed on 18 February 2024).
36. *AS 3600:2018*; Concrete Structures. Standards Australia Store: Sydney, Australia, 2018. Available online: https://store.standards.org.au/product/as-3600-2018 (accessed on 18 February 2024).